Current and Upcoming Sensitivities to Dark Matter in Gamma-Ray Observatories

J. Patrick Harding

University of Maryland

9 January 2012

Kevork Abazajian, Steve Blanchet, JPH (1011.5090)
Kevork Abazajian, Steve Blanchet, JPH (1012.1247)
Kevork Abazajian and JPH (1110.6151)

WIMP Dark Matter

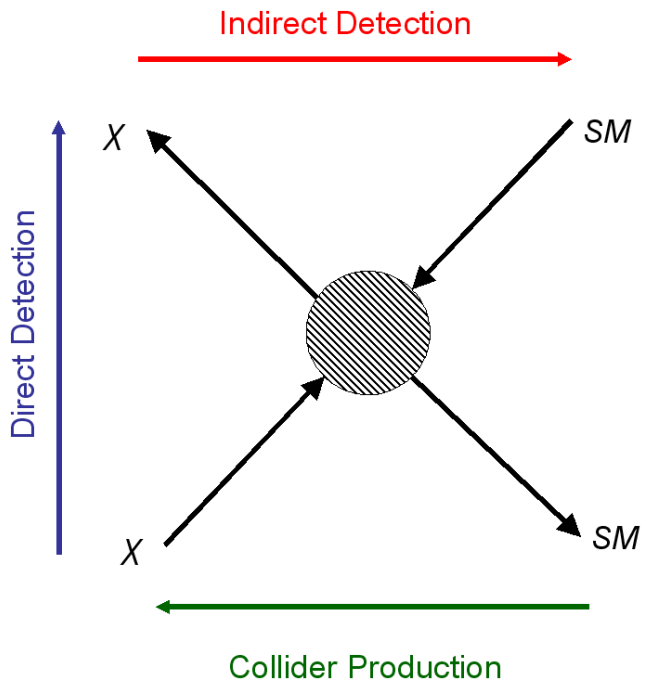

- Colliders: Produce WIMPs by colliding SM particles
- Direct Detection: Observe WIMP interaction with SM particles
- Indirect Detection: Observe SM particles produced by WIMP annihilation and decay

CDM to γ-ray: the Potential Dark Matter Sky

Springel et al. 2008

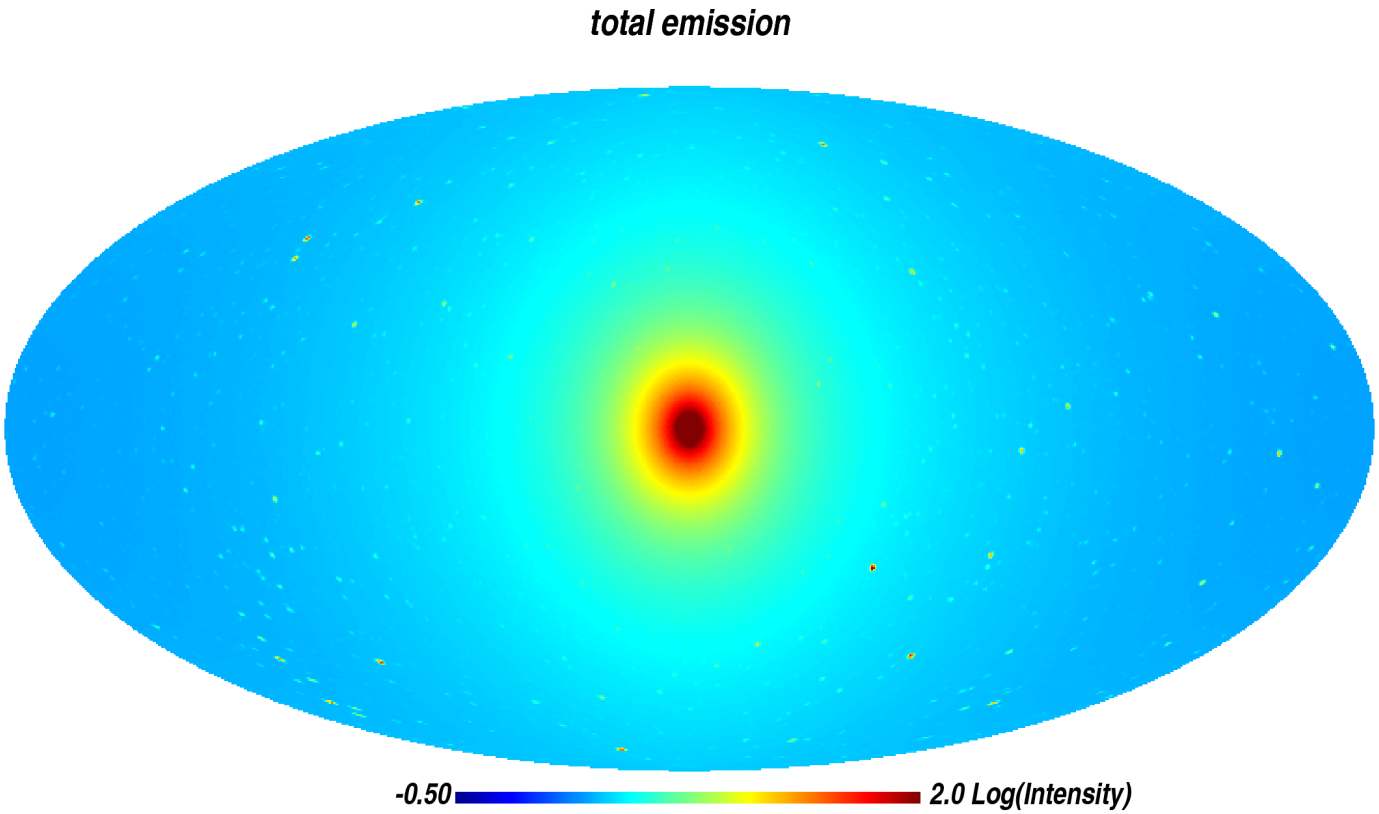

The Fermi γ-ray Sky

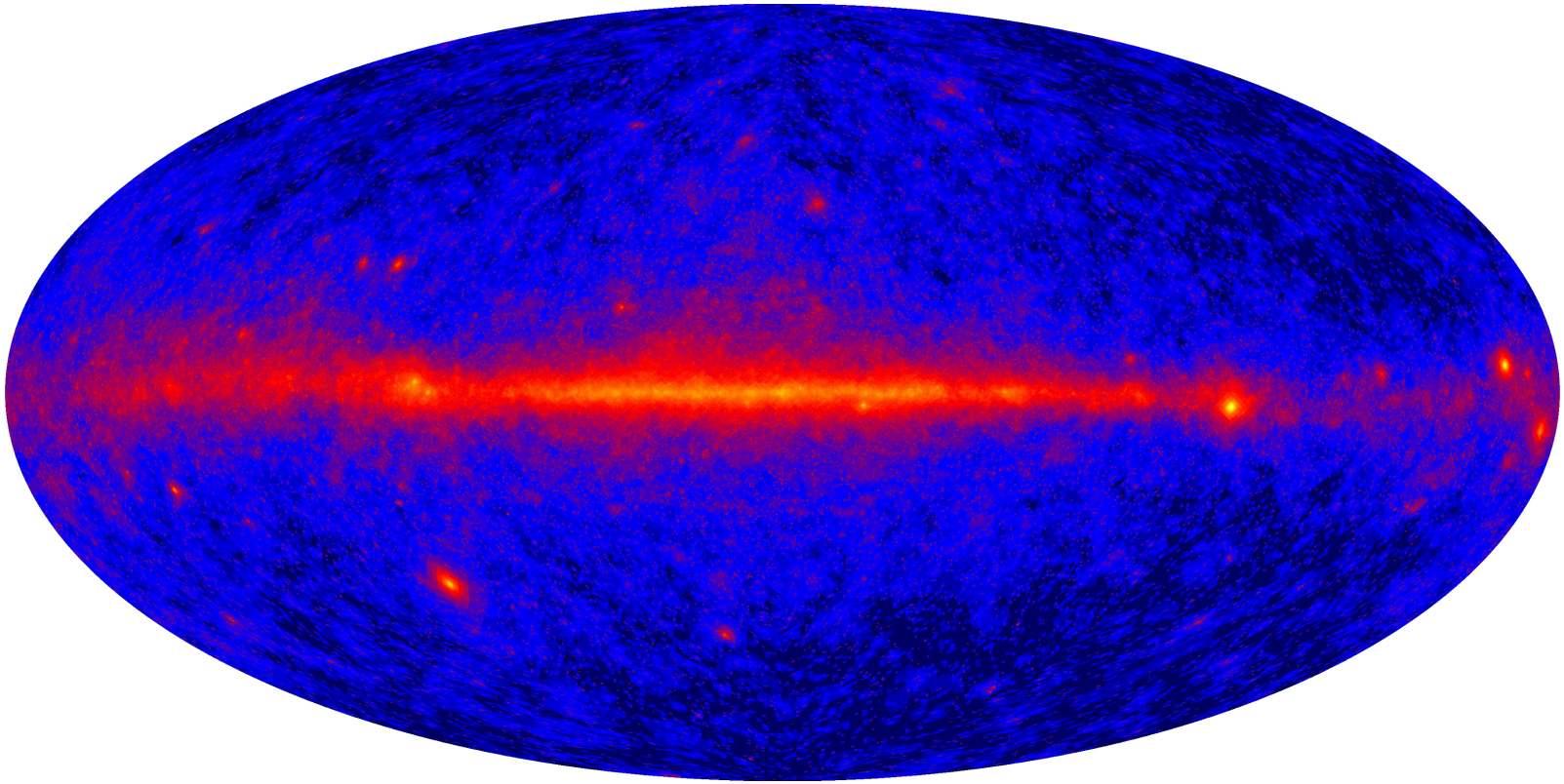

Three Types of Dark Matter Experiments

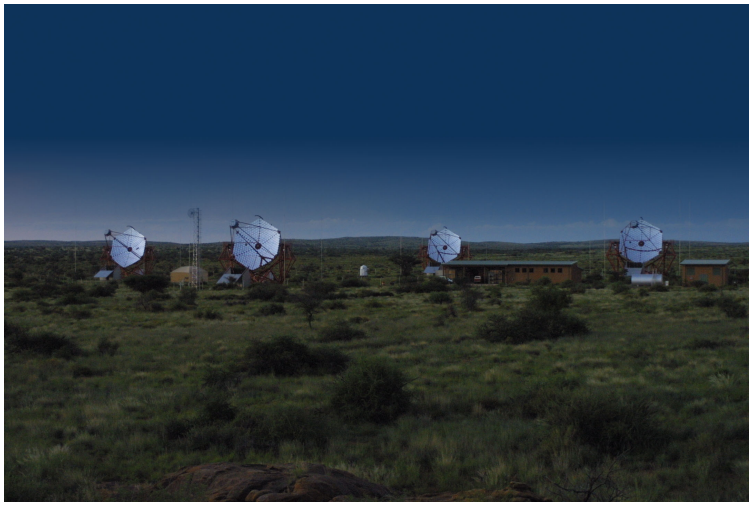

Thermal WIMPs

J. Feng

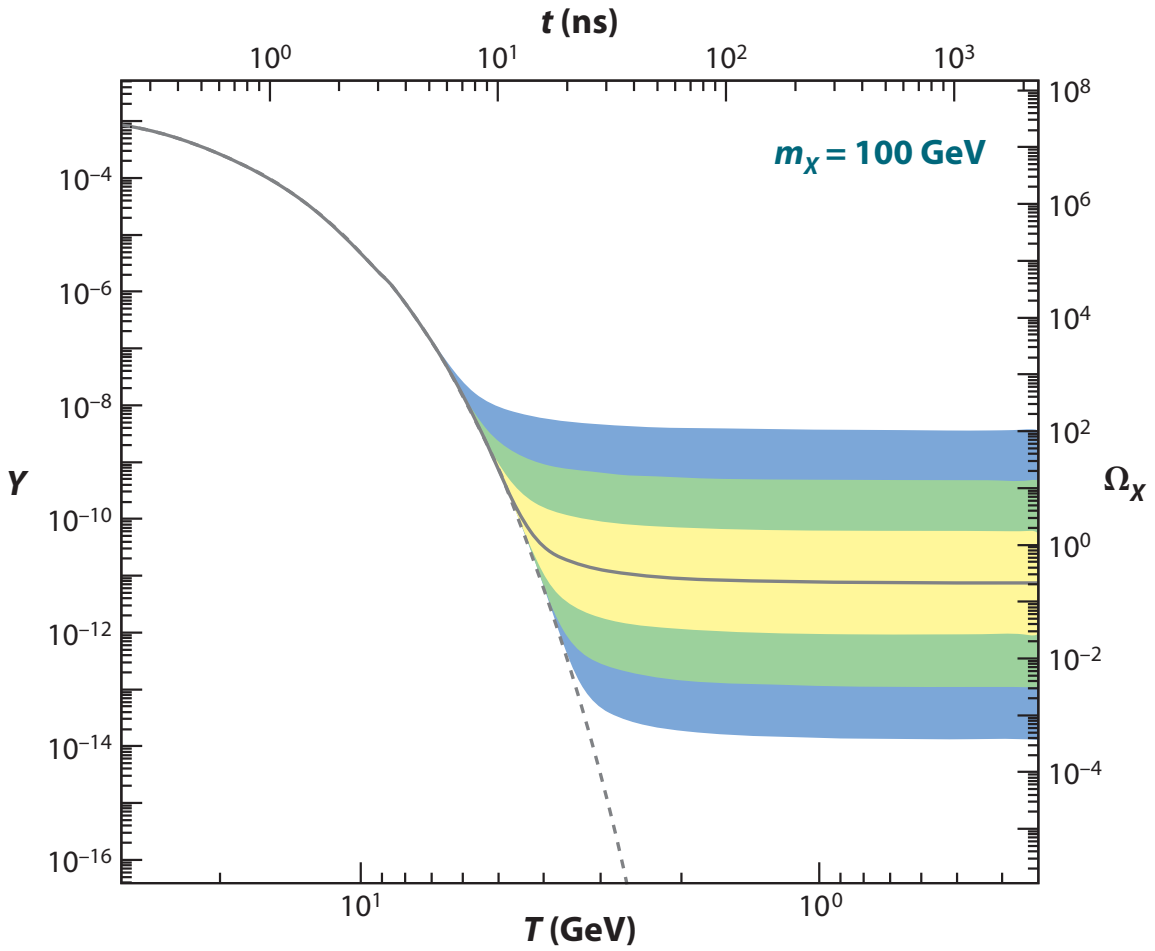

For thermal relics, $\langle \sigma v \rangle \approx 3 \times 10^{-26}\ \mathrm{cm}^3\ \mathrm{s}^{-1}$

Sommerfeld Enhancement

Slatyer et al. 2011

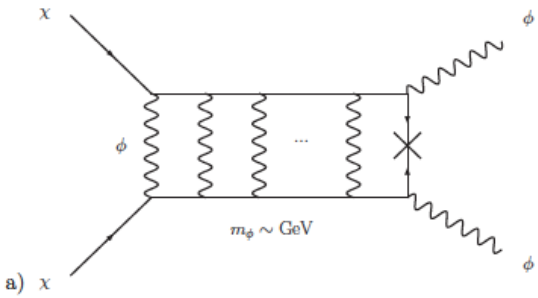

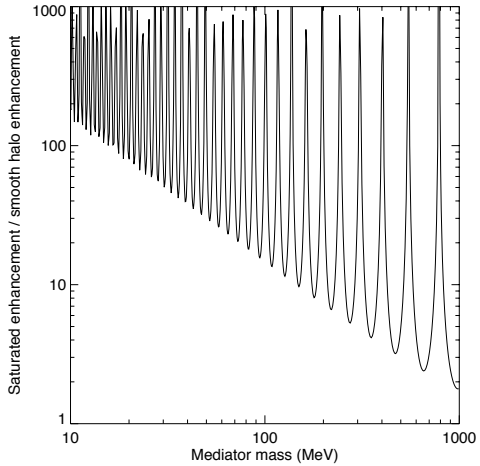

In models with light mediating bosons, low-velocity annihilations have a much higher cross-section than thermal.
In substructure, DM should have a lower velocity than in the smooth halo,so the annihilation cross-section may be boosted.

PAMELA/Fermi-LAT Positron Excess

Adriani et al. 2008; Abdo et al. 2009

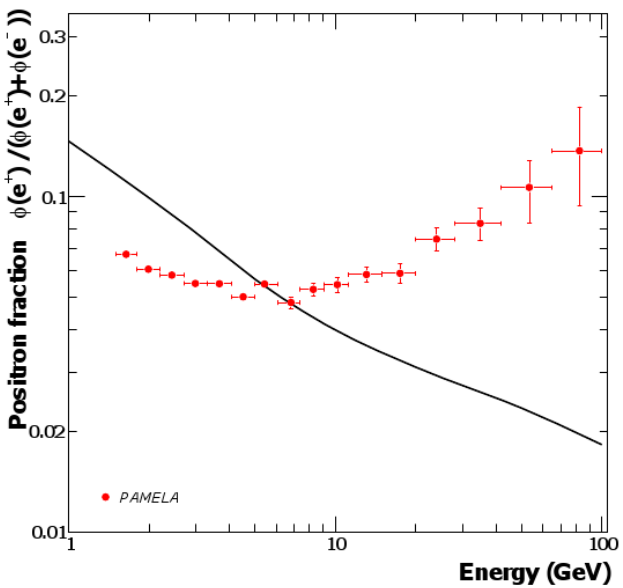

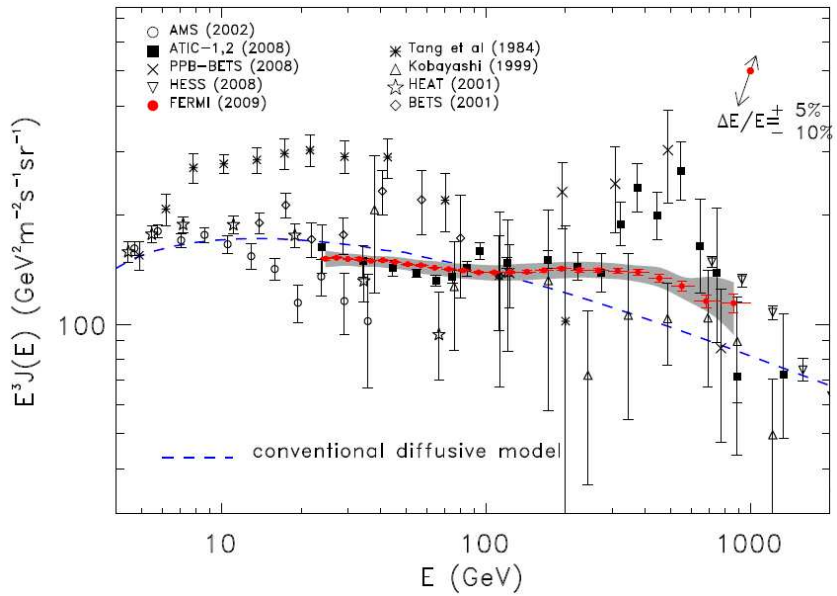

The Fermi-LAT

- Energy Resolution: $\sim$10% from $\sim 30\ \mathrm{MeV} - 300\ \mathrm{GeV}$
- Angular resolution: $\sim 0.1^\circ - 1^\circ$
- Field-of-view: 20% of the sky (8000 deg^2)
- Effective Area: $1\ \mathrm{m}^2$
- Sensitivity: $\sim 2 \times 10^{-9}\ \mathrm{cm}^{-2}\mathrm{s}^{-1} - 7 \times 10^{-8}\ \mathrm{cm}^{-2}\mathrm{s}^{-1}$

Fermi Measurement of the Diffuse Gamma-Ray Background

Abdo et al. 2010

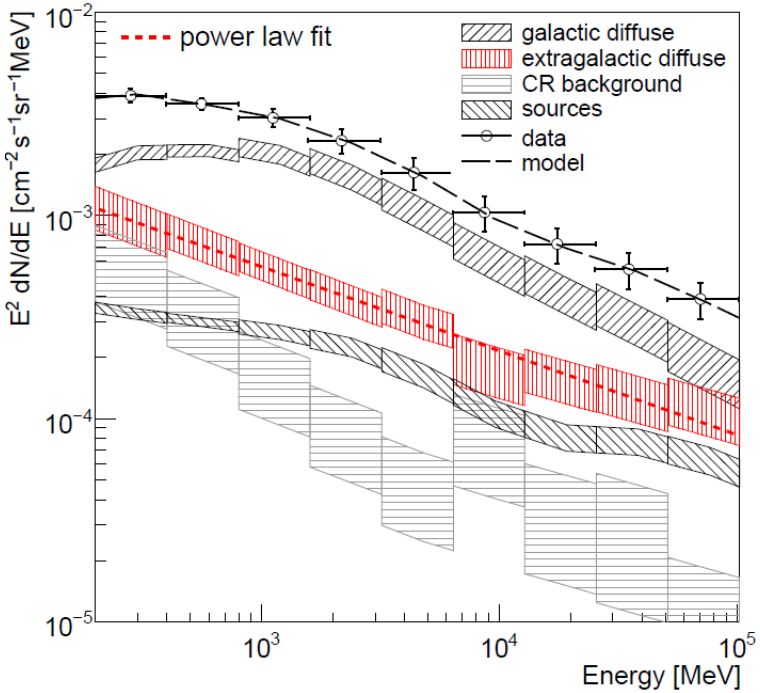

- $\sim 1/4$ of total observed flux
- Detected by subtracting galactic foregrounds
- Consists of diffuse extragalactic emission and isotropic diffuse Galactic emission

Blazars in the Unified Model of AGN

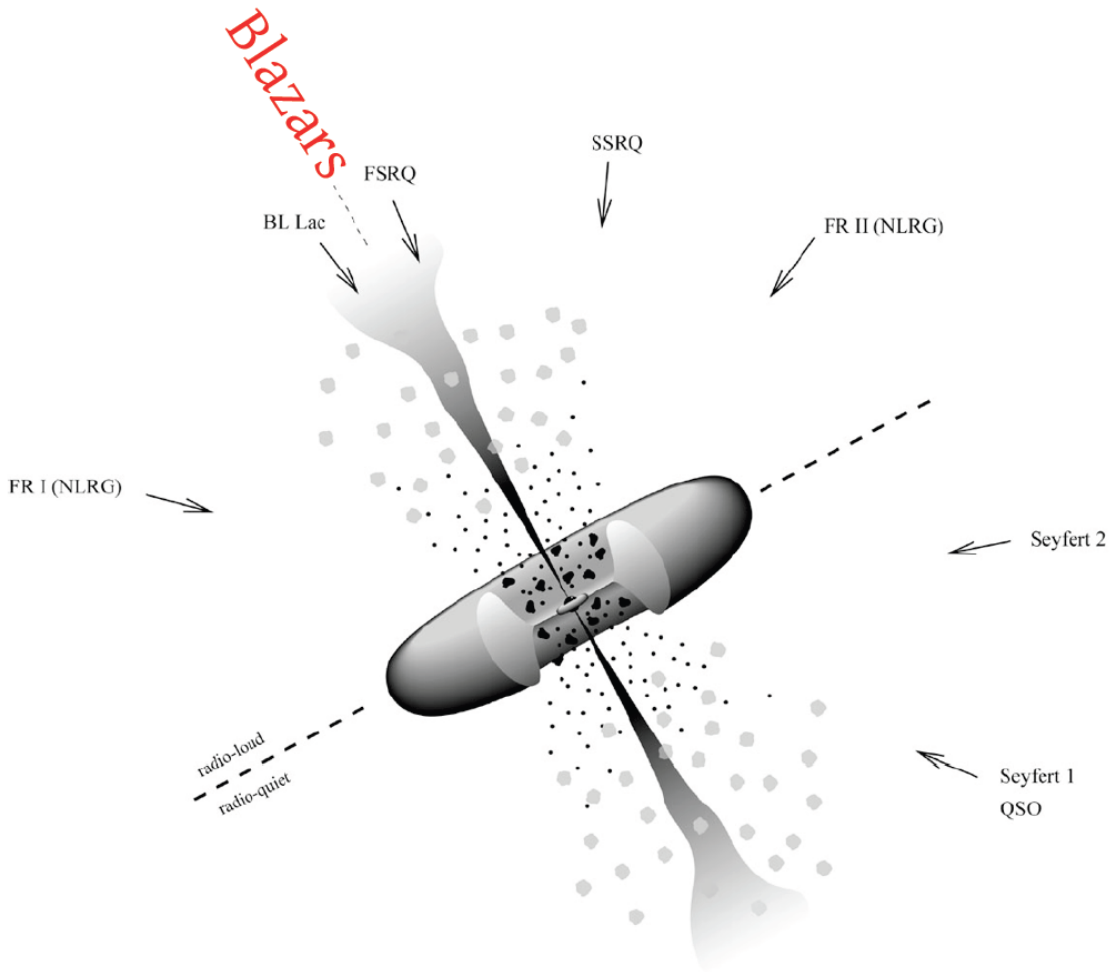

Resolved blazars make up 15% of the total Fermi-LAT emission

Blazar SED Sequence LDDE Model

- DGRB includes a contribution from non-blazar AGN at low energies (< 200 MeV)
- Blazar spectrum from a spectral energy distribution sequence
- Three parameter model for blazar evolution:
  - γ_1, the faint-end index of the GLF
  - κ, the normalization ratio of blazar GLF to AGN XLF (fraction of AGN as blazars)
  - q, scale of the blazar jet emission to disk X-ray luminosity
- We constrain this model with the observed Fermi-LAT DGRB spectrum and blazar flux multiplicity dN/dF

Spectral Energy Distribution

Donato et al. 2001

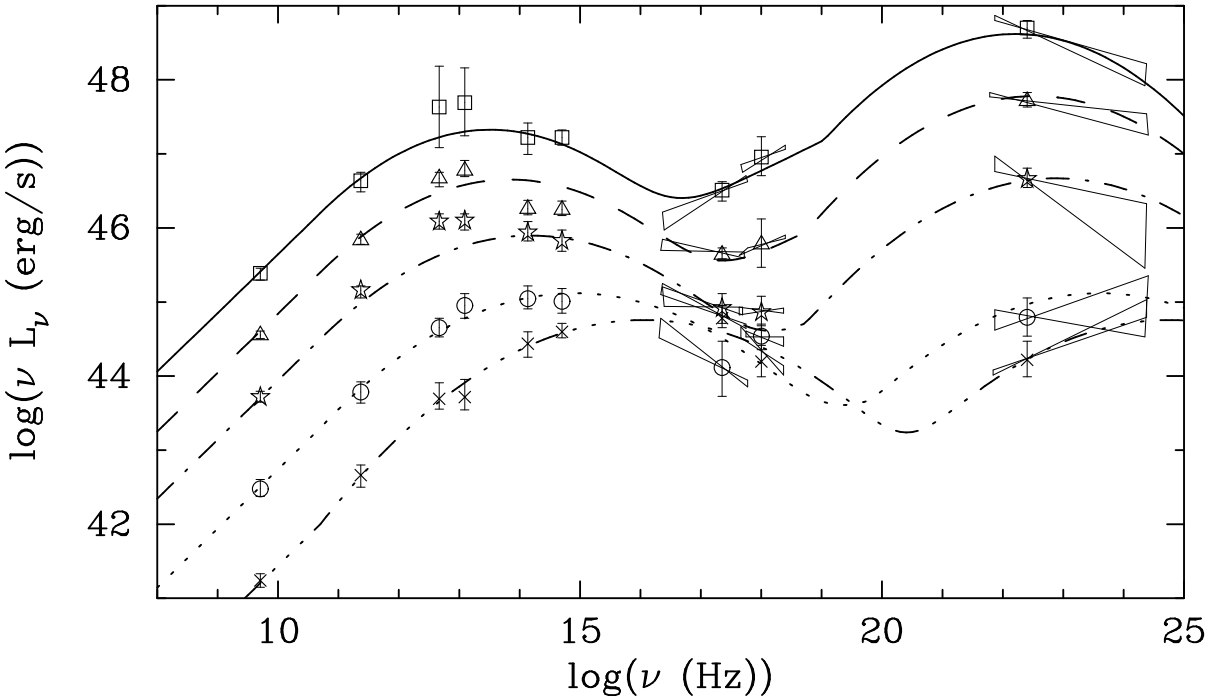

- Synchrotron component and IC component
- We follow Inoue & Totani 2008: linear and parabolic part to each component
- Luminosity-dependent slope, not gamma-ray indices

Gamma-Ray Luminosity Function

- Luminosity-dependent density evolution model for blazar density
- $\rho_X(L_X, z)$ for AGN with disk luminosity L_X parameterized by Ueda et al. 2003
- $P = 10^q L_X$ for AGN close to the Eddington limit
- $\rho_\gamma(L_\gamma, z) = \kappa \frac{dL_X}{dL_\gamma} \rho_X(L_X, z)$
- q, κ, and the faint-end index γ_1 are free parameters

Blazar Flux and dNdF

For sensitivity F_γ, the number count of detected blazars is

$$N(>F_\gamma) = 4\pi \int_0^{z_{max}} dz \frac{dV}{dz} \int_{L_\gamma^{lim}(z,F_\gamma)}^{\infty} dL_\gamma \rho_\gamma(L_\gamma, z)$$

The diffuse flux coming from unresolved blazars is given by

$$\frac{dN}{dE_\gamma dA dt d\Omega} = \frac{1}{4\pi} \int_0^{z_{max}} dz \frac{d\chi}{dz} \int_{L_{\gamma,min}}^{L_\gamma^{lim}(F_\gamma,z)} dL_\gamma \rho_\gamma(L_\gamma, z) \times \frac{1}{h} \frac{L_\nu[E_\gamma(1+z)/h, P(L_\gamma)]}{E_\gamma} e^{-\tau(z,E_\gamma)}$$

Unresolved Blazars Form the DGRB

- We do simultaneous fit to dN/dF and the DGRB
- Best-fit parameters $q = 4.19^{+0.57}_{-0.13}$, $\gamma_1 = 1.51^{+0.10}_{-0.09}$, $log(\kappa/10^{-6}) = 0.38^{+0.15}_{-0.70}$ $(\kappa = 2.4 \times 10^{-6})$
- Good fit to data, with $\chi^2/\mathrm{DOF} = 0.63$
- Sensitivity given by:

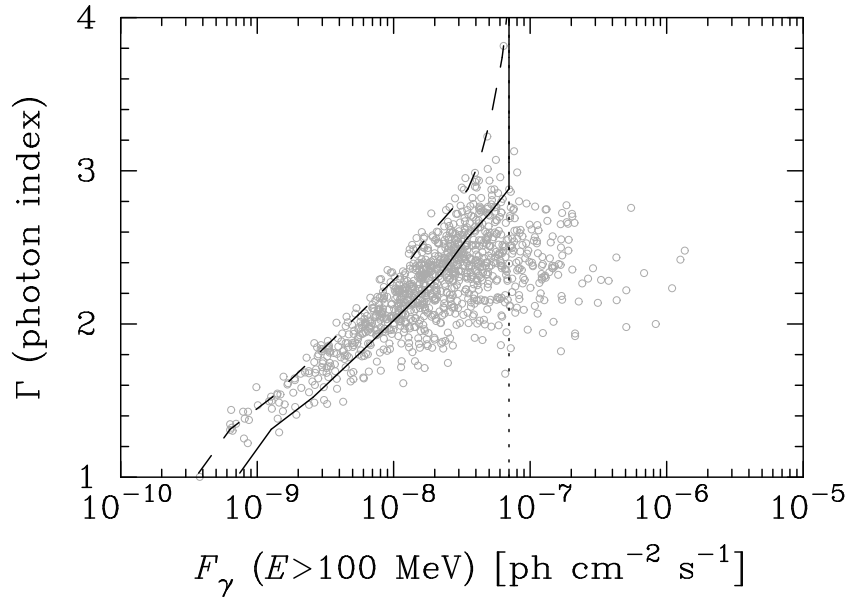

Blazar Predictions

Abazajian, Blanchet, JPH 2010

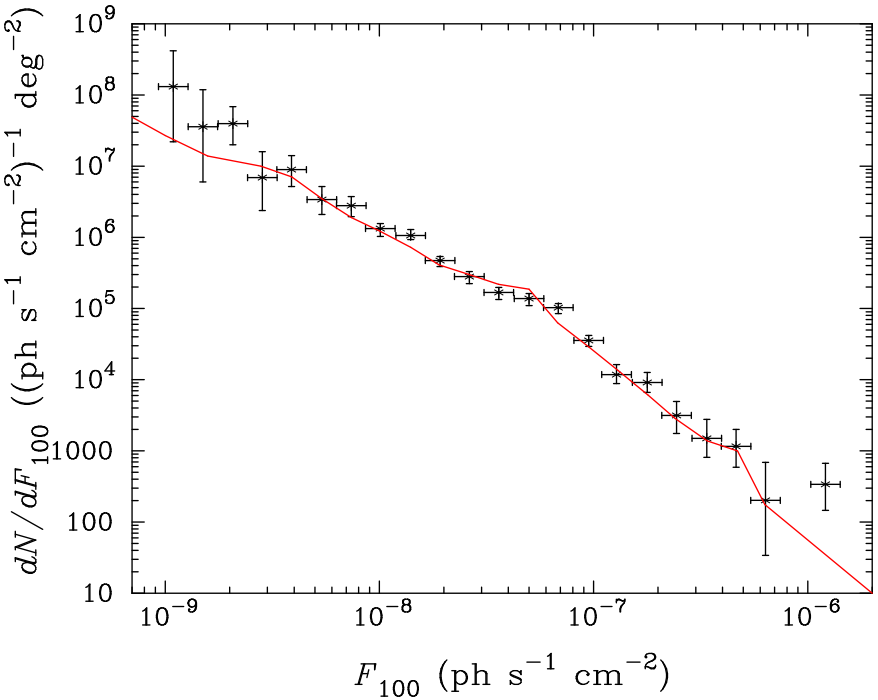

- Made predictions for Fermi-LAT 5-year sensitivity
- $94.7^{+1.9}_{-2.1}$ % of total blazar flux resolved
- 2415^{+240}_{-420} blazars resolved, of $5.4^{+1.8}_{-1.7} \times 10^4$ total blazars

Predicted 5-year Fermi-LAT DGRB

Abazajian, Blanchet, JPH 2010

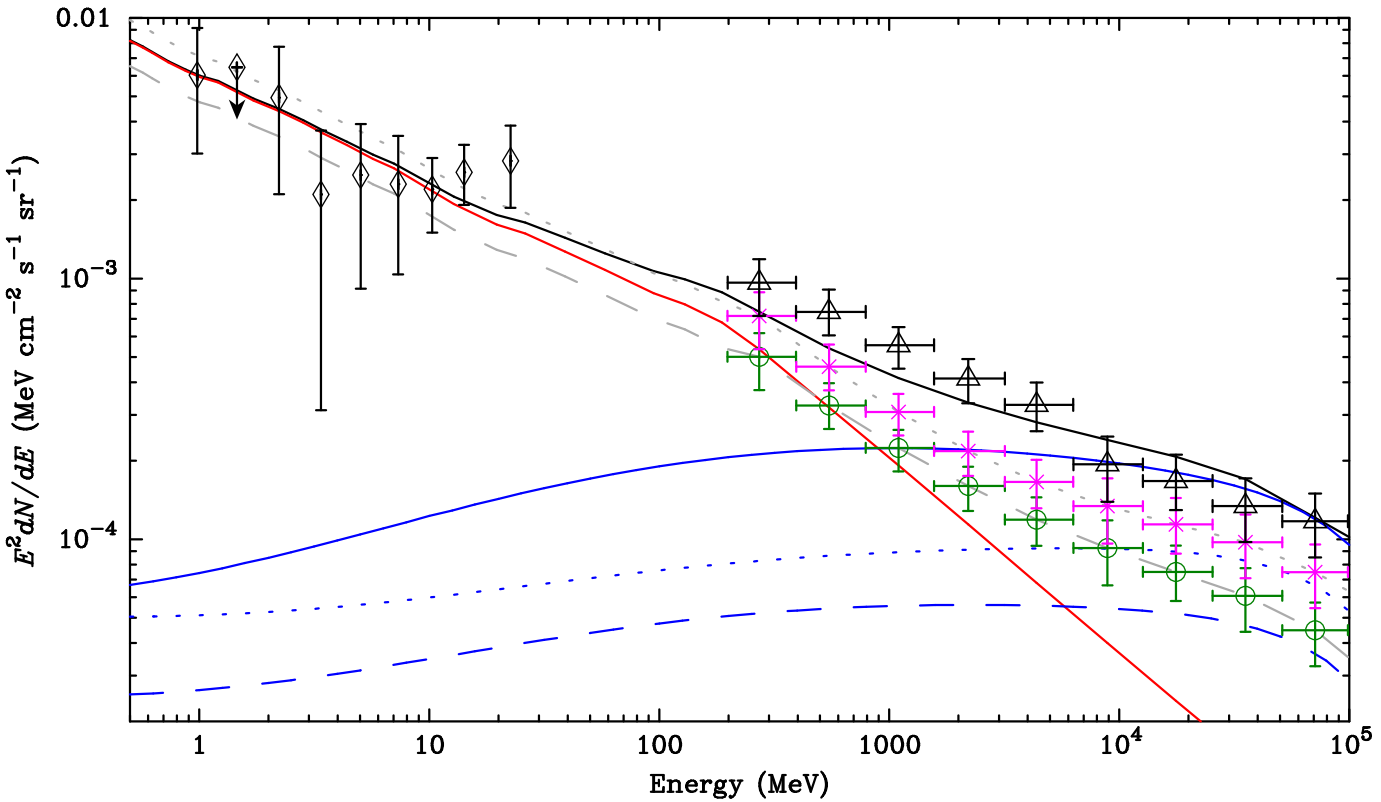

- Solid blue line is the current blazar component of the DGRB
- Dotted (dashed) blue lines are the most (least) optimistic 95% CL 5-year Fermi-LAT blazar contributions
- Red, non-blazar AGN component from Inoue et al. 2007
- COMPTEL data (diamonds) from Watanabe et al. 2003

Dark Matter Annihilation

The Galactic contribution to the gamma-ray flux is given by:

$$\frac{dF_\gamma}{dEd\Omega} = \frac{\langle\sigma_A v\rangle}{2}\frac{\mathcal{J}_{\Delta\Omega}}{\mathrm{J}_0}\frac{1}{4\pi m_\chi^2}\frac{dN_\gamma}{dE}$$

$$\mathcal{J}_{\Delta\Omega} = \frac{\mathrm{J}_0}{\Delta\Omega_{\mathrm{obs}}}\int_{\Delta\Omega_{\mathrm{obs}}} d\Omega \int_{x_{\mathrm{min}}}^{x_{\mathrm{max}}} dx\, \rho^2\left(r_{\mathrm{gal}}(b,\ell,x)\right)$$

For diffuse flux, we use $(b,\ell) = (0^\circ, 180^\circ)$.
The extragalactic contribution to the diffuse flux is given by:

$$\frac{dF_\gamma}{dEd\Omega} = \frac{\langle\sigma_A v\rangle}{2}\frac{c}{4\pi H_0}\frac{(f_{\mathrm{DM}}\Omega_m)^2\rho_{\mathrm{crit}}^2}{m_\chi^2} \times \int_0^{z_{\mathrm{up}}} \frac{f(z)(1+z)^3 e^{-\tau(z,E')}}{\sqrt{(1+z)^3\Omega_m + \Omega_\Lambda}}\frac{dN(E')}{dE'}dz$$

$b\bar{b}$ WIMP Annihilation Channel Constraints from the Fermi-LAT DGRB

Abazajian, Blanchet, JPH 2010

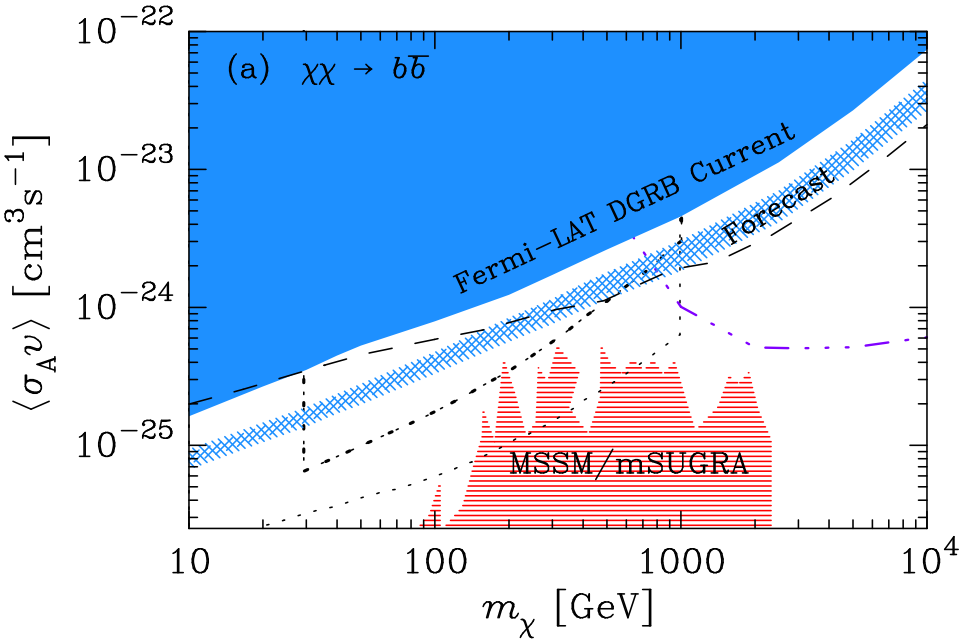

Solid (hashed) blue regions show the limits from the current (predicted) Fermi-LAT DGRB measurements.
Thick dotted line is limit from Fermi-LAT observations of Draco from Abdo et al. 2010
Thin dotted line is limit from stacked Fermi-LAT dwarf galaxy observations from Ackermann et al. 2011
Dashed Fermi-LAT 3σ limits from inner $3^\circ \times 3^\circ$ of MW from Cirelli et al. 2010
Triple-dot-dashed limits from HESS observations of the Galactic center from Abazajian & JPH 2011
The red-striped region shows a sampling of points in SUSY parameter space from Bergstrom et al. 2010

$\mu^+\mu^-$ WIMP Annihilation Channel Constraints from the Fermi-LAT DGRB

Abazajian, Blanchet, JPH 2010

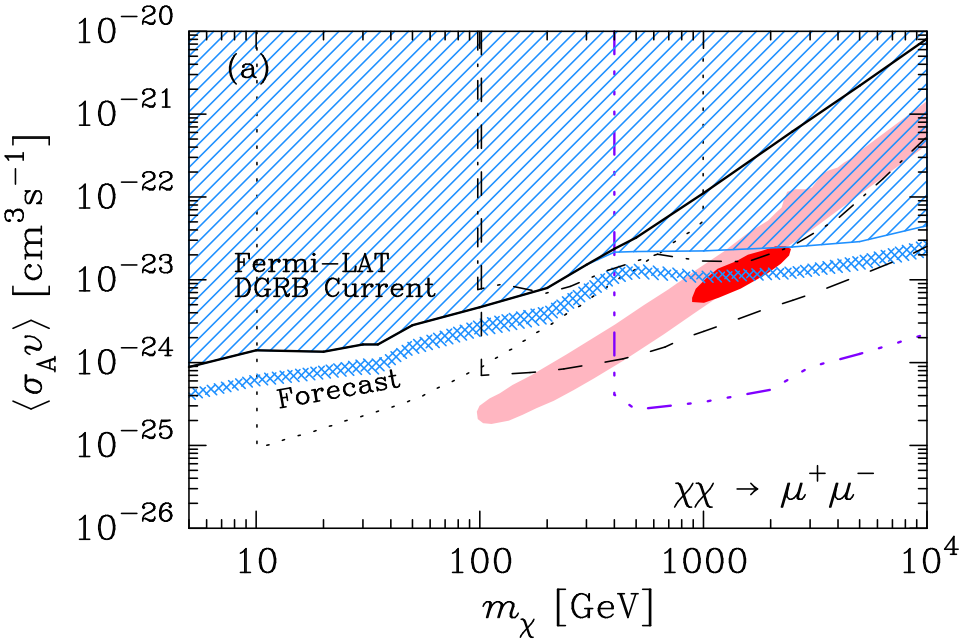

Striped (hashed) blue regions show the limits from the current (predicted) Fermi-LAT DGRB measurements
The solid black line shows where the exclusion would be without the Inverse Compton contribution
The dot-dashed line is the 95% CL limit on prompt and IC emission from Ursa Minor from Abdo et al. 2010
Triple-dot-dashed limits from HESS observations of the Galactic center from Abazajian & JPH 2011
The dotted line is a limit from radio synchrotron from the Galactic center from Meade et al. 2010
Dashed Fermi-LAT 3σ limits from inner $3^\circ \times 3^\circ$ of MW from Cirelli et al. 2010
Pink (red) PAMELA (Fermi-LAT) excess regions from Mead et al. 2010

Fermi-LAT Stacked Dwarf Analysis

Geringer-Sameth & Koushiappas 2011; Ackermann et al. 2011

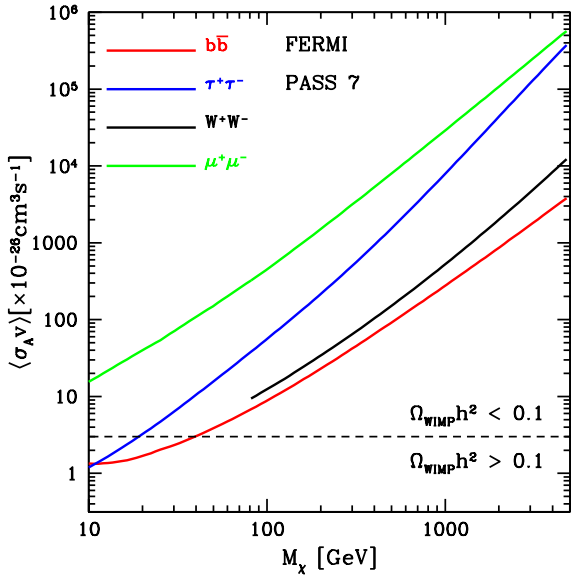

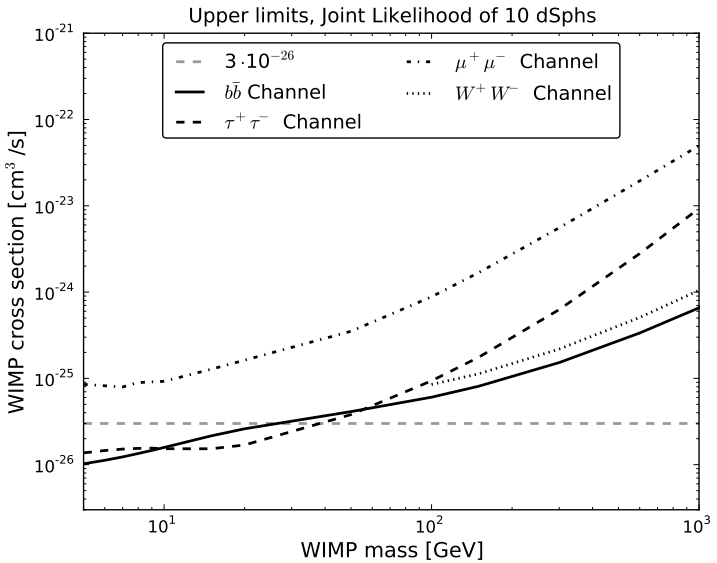

Geringer-Sameth & Koushiappas considers 7 dwarf spheroidal galaxies

Ackermann et al. considers 10 dwarf spheroidal galaxies

Thermal $b\bar{b}$ ($\tau^+\tau^-$) channel WIMPs are excluded below ~ 35 GeV (20 GeV)

Galactic Center Limits from Annuli

Baxter & Dodelson 2011

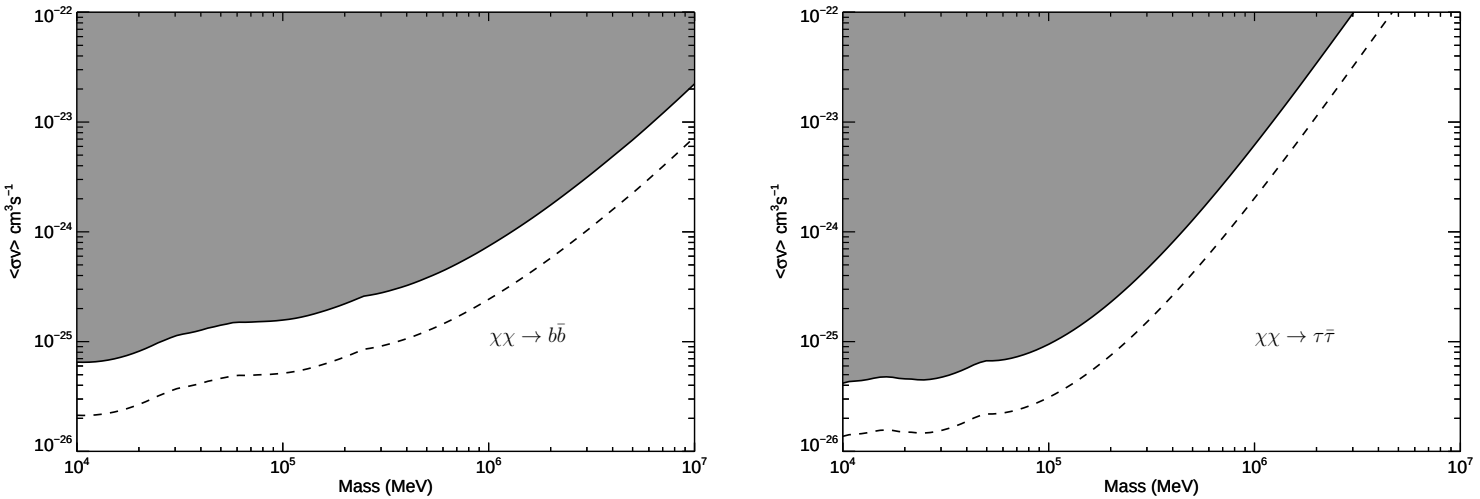

Used "independent and identically distributed" annuli around the GC.

Uncertainties are due to shape of DM halo profile.

Comparable to results from Fermi-LAT dwarfs.

Fermi-LAT Galactic Center Analysis

Hooper & Linden 2011

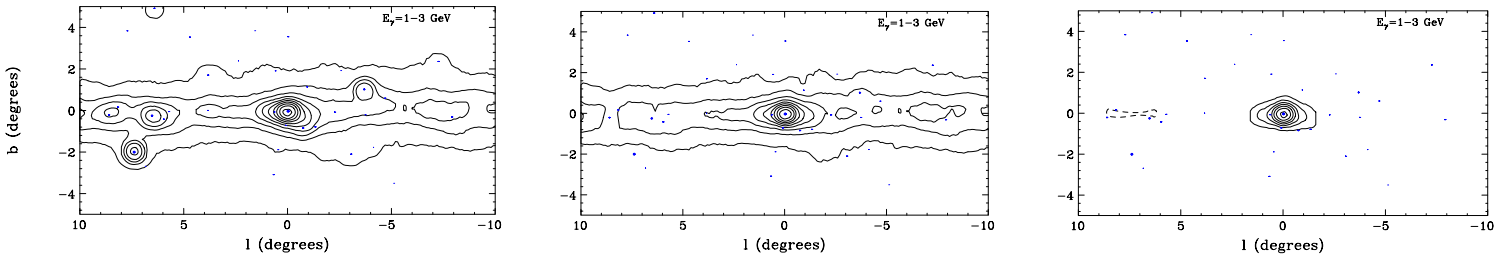

Fermi-LAT GC 1-3 GeV flux, emission with point sources removed, and emission with gas template and point sources removed.

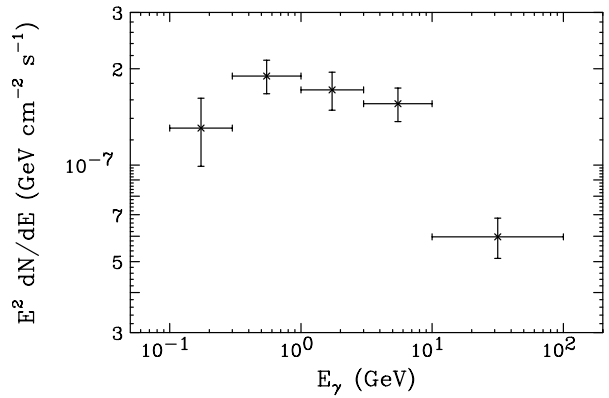

The residual emission peaks strongly toward the GC and peaks in energy at ~ 1 GeV.

Dark Matter Signal from the Fermi-LAT Galactic Center Analysis

Hooper & Linden 2011

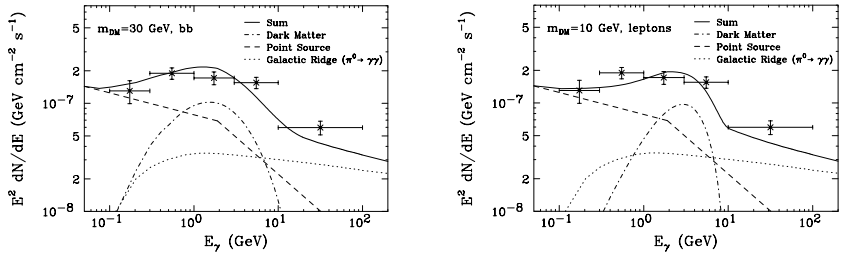

The residual GC signal fits a dark matter annihilation signal for a light WIMP with a $r^{-1.3}$ dark matter density profile.

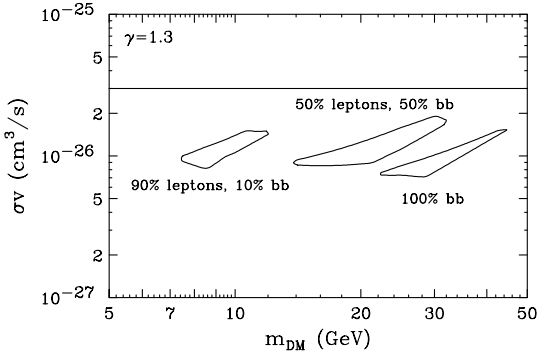

The dark matter annihilation spectrum fits either a $b\bar{b}$ or $\tau^+\tau^-$ annihilation channel, with a cross-section that is 20-50% of thermal.

Dark Matter Limits from the Fermi-LAT Galactic Center Analysis

Hooper & Linden 2011

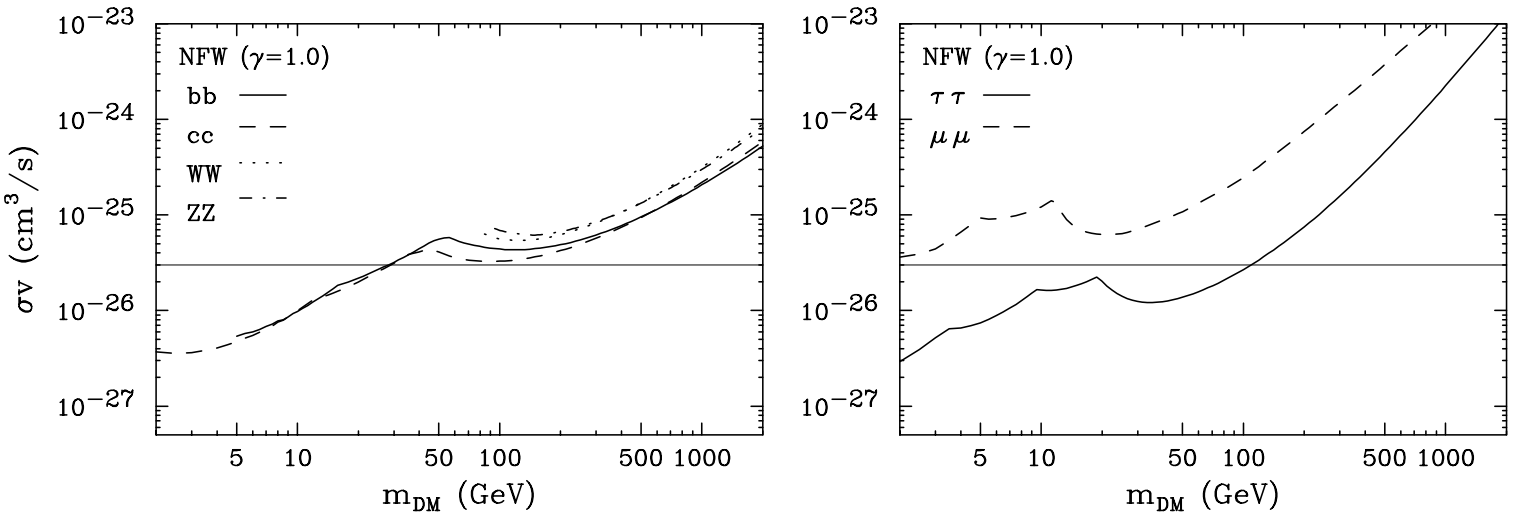

Limits from the Fermi-LAT GC analysis for an NFW DM profile.

Thermal $b\bar{b}$ is excluded above ~ 30 GeV.

Thermal $\tau^+\tau^-$ is excluded above ~ 100 GeV.

The High Energy Stereoscopic System

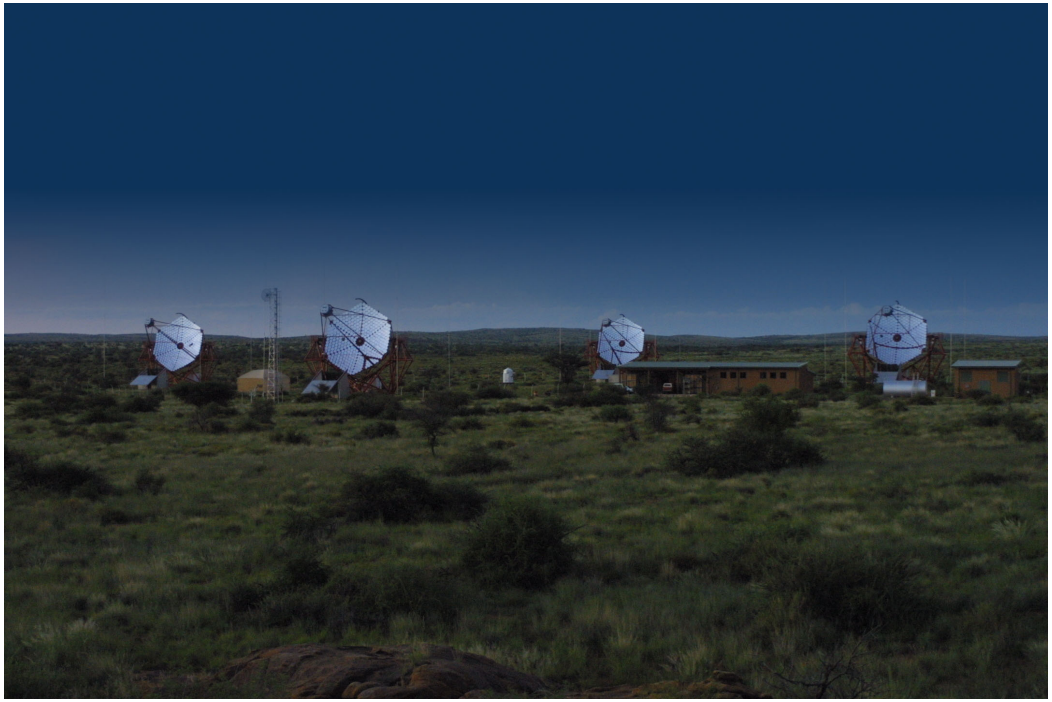

- Energy Resolution: $\sim$15% from $\sim 100\ \mathrm{GeV} - 10\ \mathrm{TeV}$
- Angular resolution: $\sim 0.1^{\circ}$
- Field-of-view: $5^{\circ} \times 5^{\circ}$
- Effective Area: $10^5\ \mathrm{m}^2$
- Sensitivity: $\sim 10^{-13}\ \mathrm{cm}^{-2}\mathrm{s}^{-1} - 10^{-11}\ \mathrm{cm}^{-2}\mathrm{s}^{-1}$

HESS Galactic Center Regions

Abramowski et al. 2011

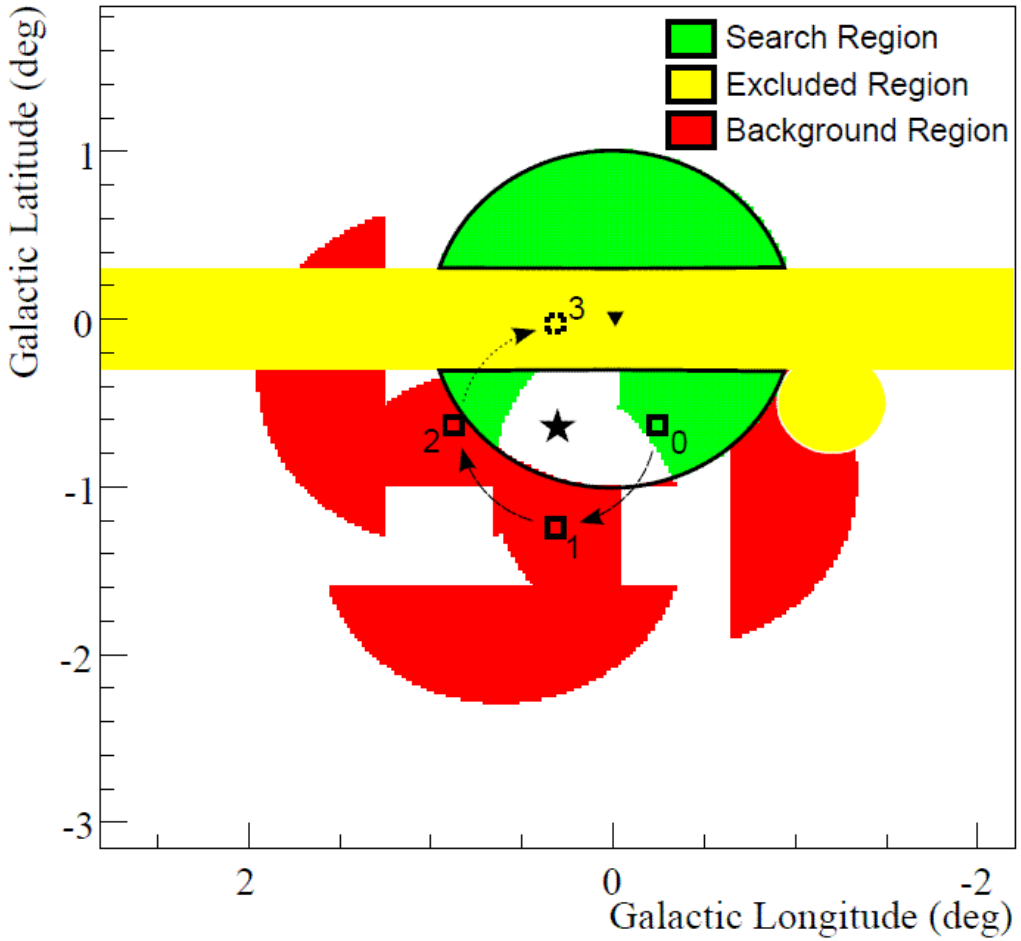

$|b| \leq 0.3^\circ$ and HESS J1745-303 have been masked

HESS Measured Fluxes

Abramowski et al. 2011

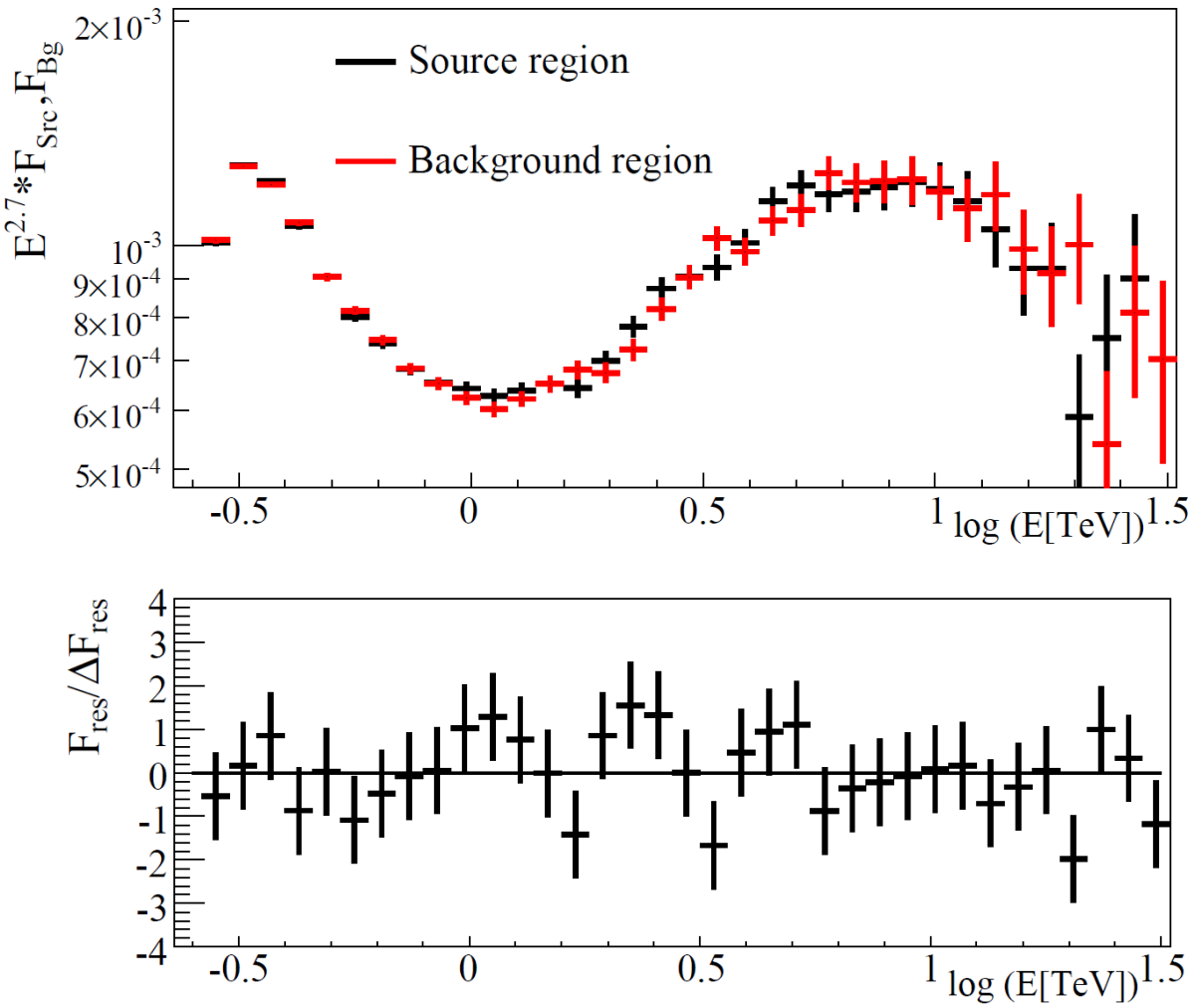

Dark Matter Density Profiles

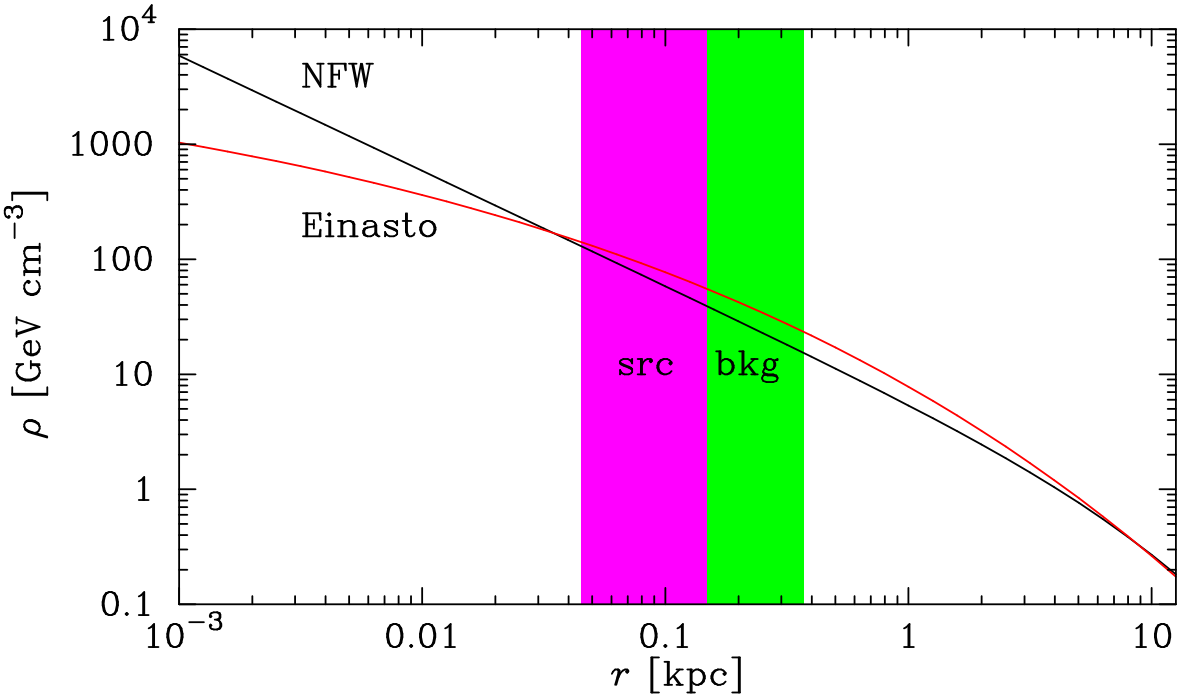

Limits are found from the difference $(dF/dE)_{src} - (dF/dE)_{bgd}$. For the angular scales considered in the HESS measurements, the NFW profile is more conservative than the Einasto profile.

Measured Fluxes vs. Dark Matter

Abazajian and JPH 2011

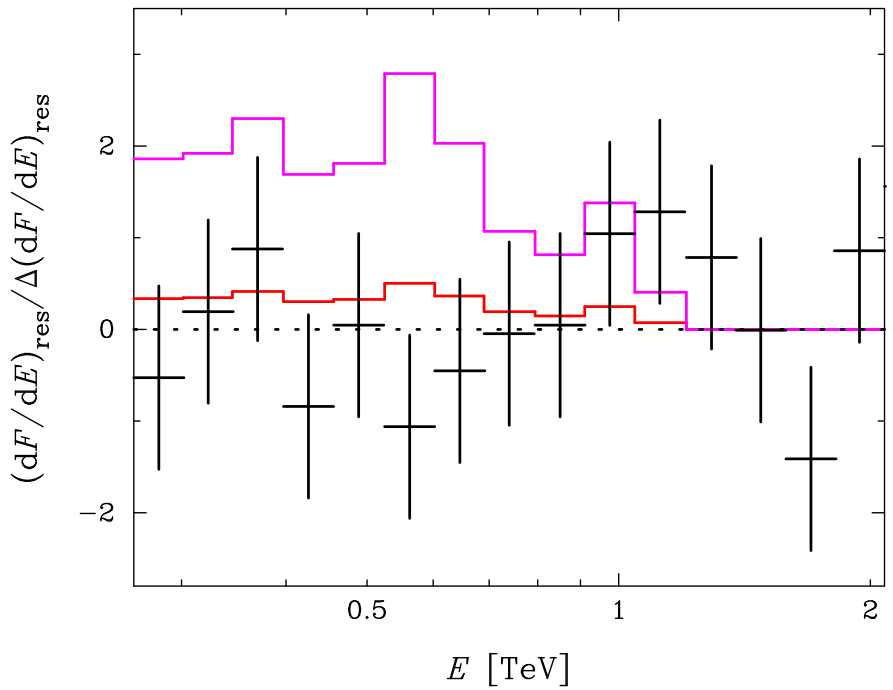

Dark matter curves are for a 1.2 TeV WIMP annihilating into two e^+e^- pairs via 0.25 GeV scalars.

The red curve is for $\langle \sigma v \rangle = 9 \times 10^{-25}\ \mathrm{cm}^3\ \mathrm{s}^{-1}$ and the magenta curve is for

$\langle \sigma v \rangle = 5 \times 10^{-24}\ \mathrm{cm}^3\ \mathrm{s}^{-1}$, both for NFW dark matter profiles.

$b\bar{b}$ WIMP Annihilation Channel Constraints from the HESS GC Observations

Abazajian and JPH 2011

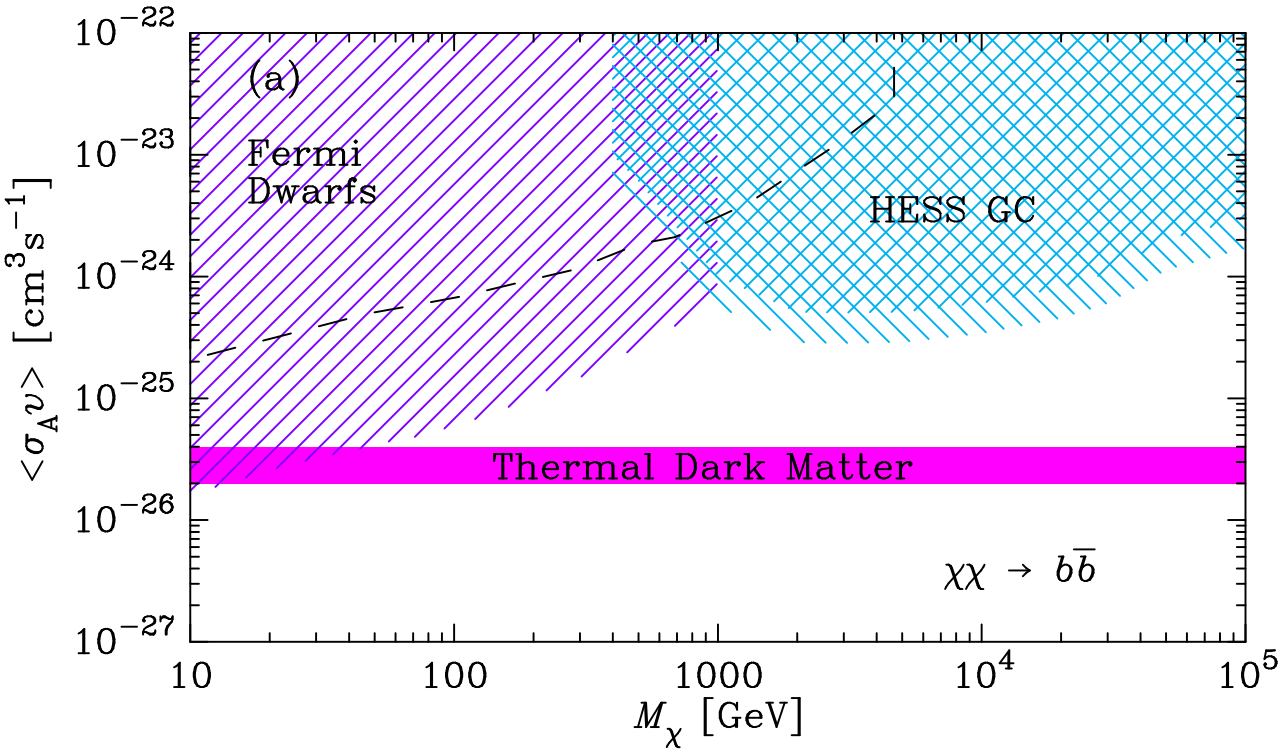

Fermi dwarf regions from Ackermann et al. 2011

Dashed Fermi-LAT 3σ limits from inner $3^\circ \times 3^\circ$ of MW from Cirelli et al. 2010

$\tau^+\tau^-$ WIMP Annihilation Channel Constraints from the HESS GC Observations

Abazajian and JPH 2011

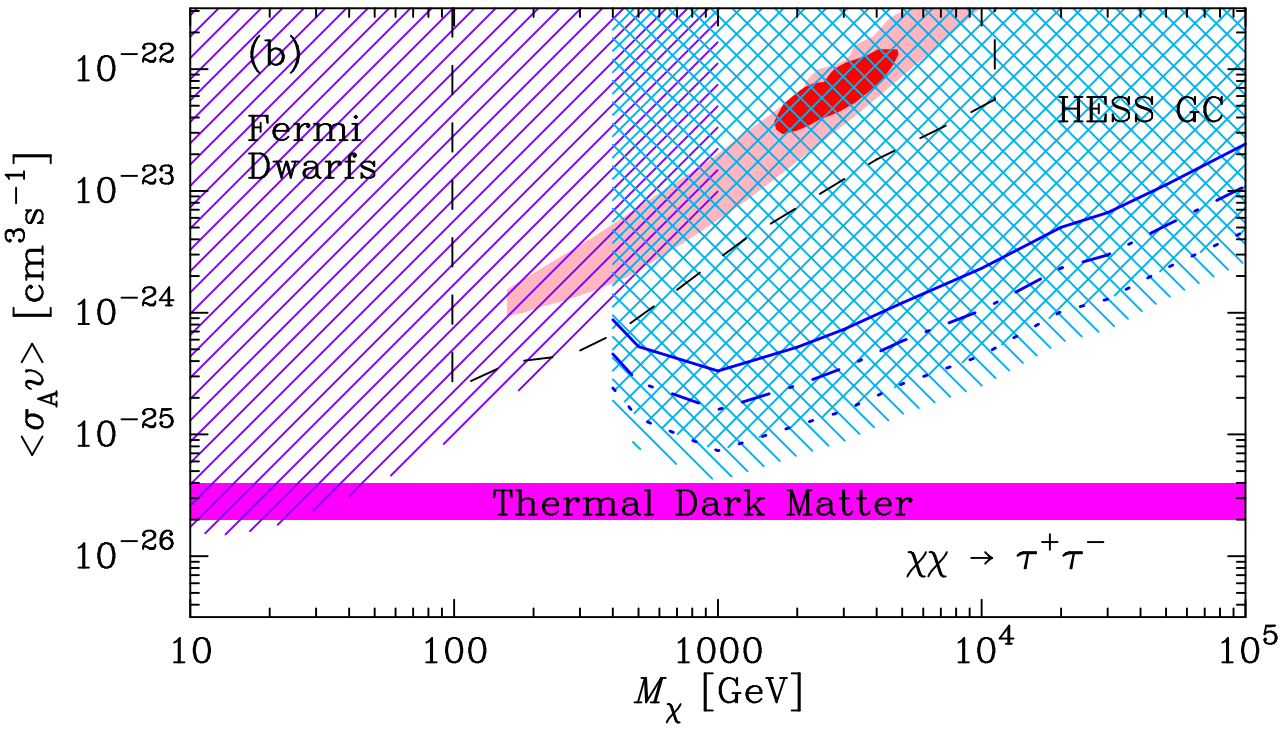

Pink (red) PAMELA (Fermi-LAT) excess regions from Mead et al. 2010

Fermi dwarf regions from Ackermann et al. 2011

Dashed Fermi-LAT 3σ limits from inner $3^\circ \times 3^\circ$ of MW from Cirelli et al. 2010

For the HESS GC limits, the 95%, 99.7%, and 99.9999% CL limits are shown.

Scalar-Mediated 4e WIMP Annihilation Channel Constraints from the HESS GC Observations

Abazajian and JPH 2011

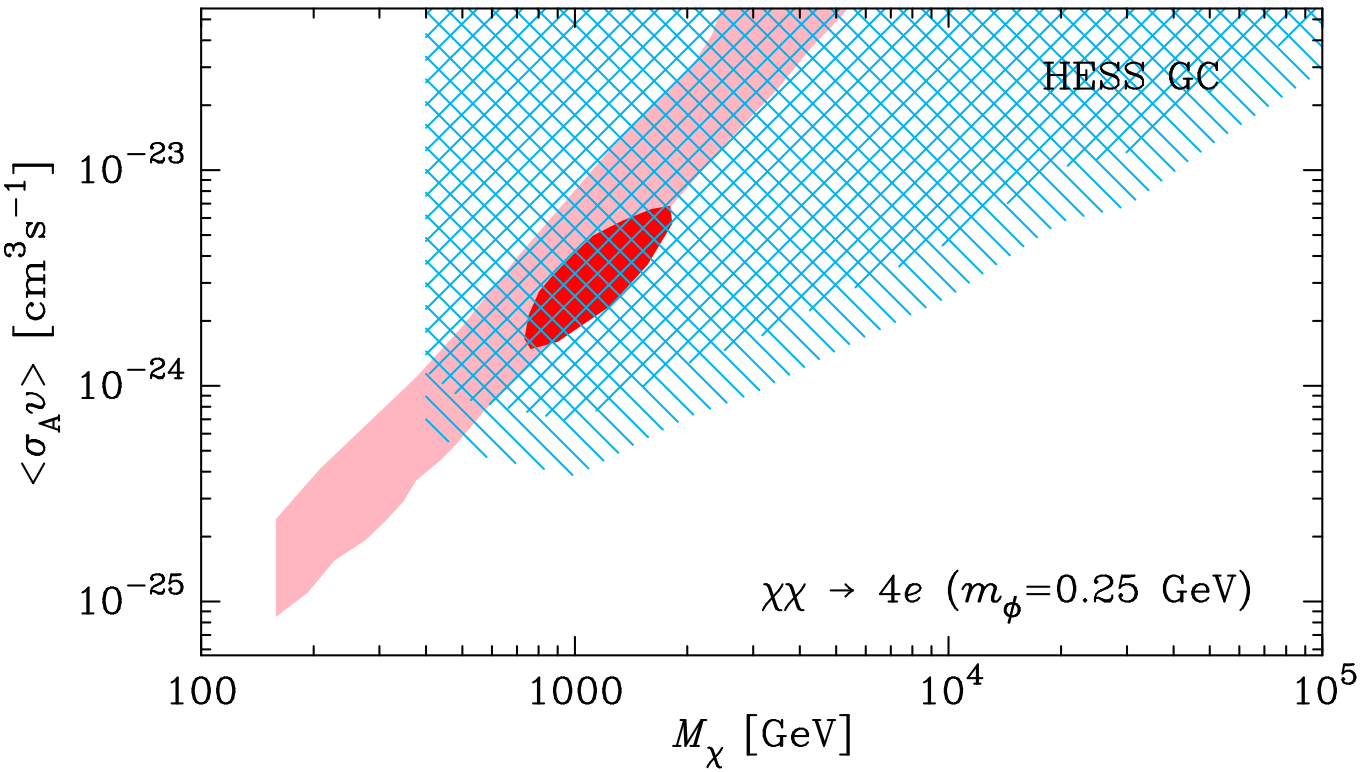

Pink (red) PAMELA (Fermi-LAT) excess regions from Mead et al. 2010

Sommerfeld-Enhanced Annihilation Channel Constraints from the HESS GC Observations

Abazajian and JPH 2011

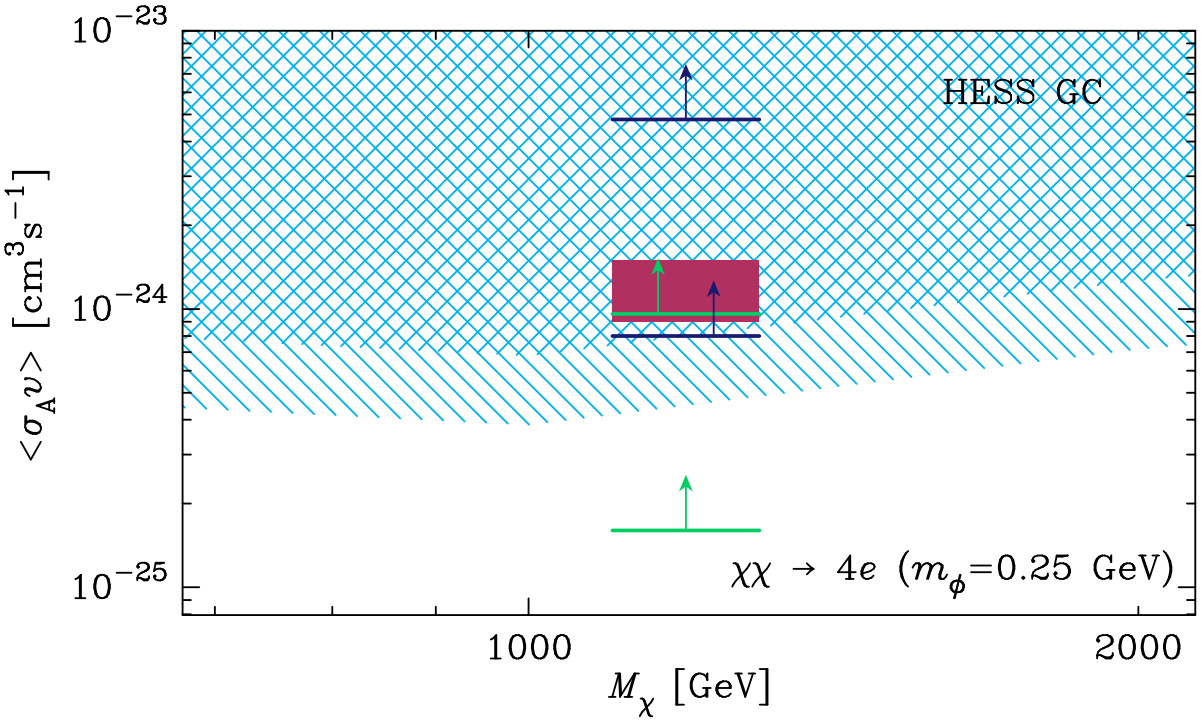

The purple region shows valid boost factors for substructure boosts from 1.0001 to two from Slatyer, Toro, and Weiner 2011. The green (blue) bars show the $v_{\rm GC} \rightarrow 0$ ($v_{\rm GC} \sim 150$ km s^{-1}) constraints for an NFW profile with these substructure boosts

XDM Annihilation Channel Constraints from the HESS GC Observations

Abazajian and JPH 2011

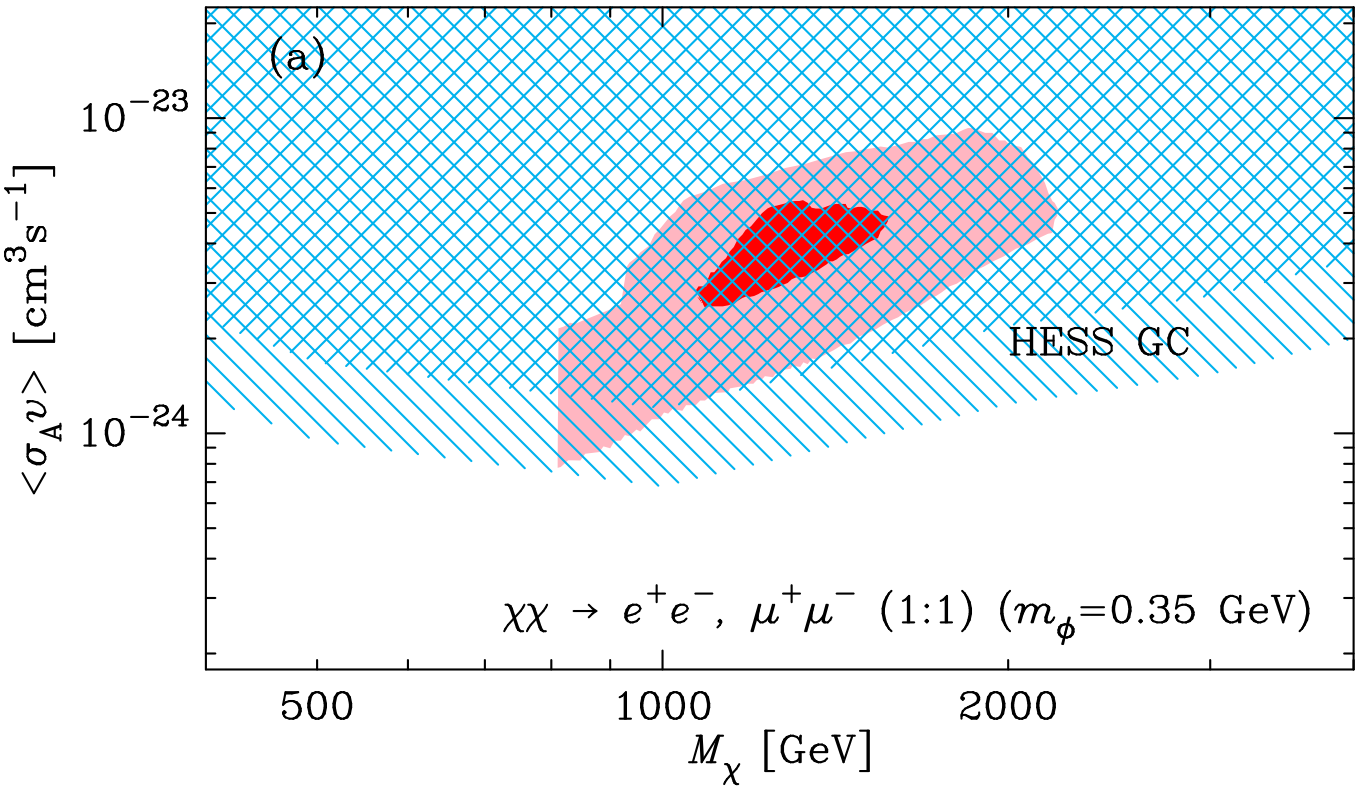

Pink (red) regions consistent at 68% CL (95% CL) for a combined

PAMELA + Fermi-LAT excess from Finkbeiner et al. 2010

The High-Altitude Water Cherenkov Gamma-Ray Observatory

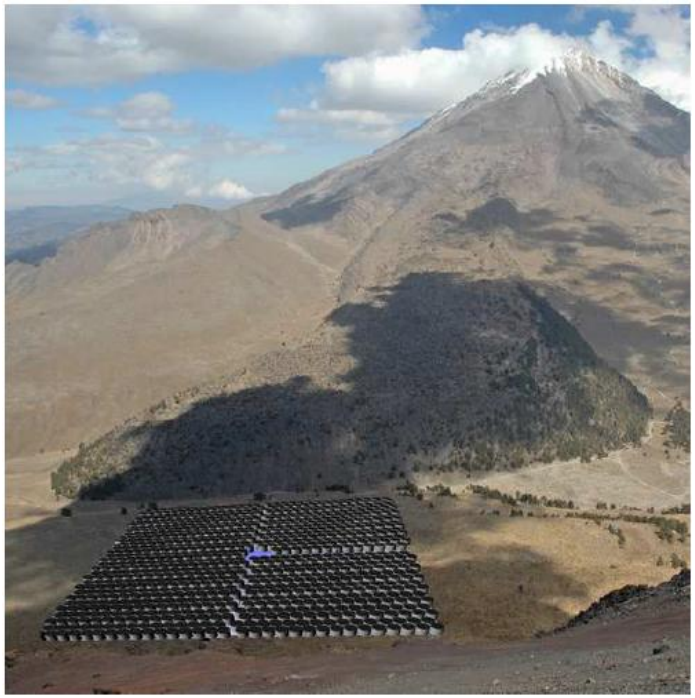

- Energy Resolution: $\sim 50\%$ from ~ 1 TeV $- 100$ TeV
- Angular resolution: $\sim 0.25^\circ - 0.5^\circ$
- Field-of-view: 1.9 sr (6000 deg^2)
- Effective Area: $10^4 - 10^5$ m^2
- Sensitivity: $\sim 10^{-14}$ $\mathrm{cm}^{-2}\mathrm{s}^{-1} - 10^{-12}$ $\mathrm{cm}^{-2}\mathrm{s}^{-1}$

HAWC Sensitivity to Dark Matter

- HAWC site is Sierra Negra, Mexico (latitude 19°N)
- Galactic Center (Dec= $-29°$) is within F.o.V., but barely
- Coma Berenices dwarf galaxy (Dec= 24°) is nearly overhead, but has a small DM *J*-factor: $\mathcal{J} \approx 1.6 \times 10^{18}\ \mathrm{GeV^2 cm^{-5}}$
- Draco dwarf galaxy (Dec= 58°) is toward the horizon, but has a large DM *J*-factor: $\mathcal{J} \approx 1.2 \times 10^{19}\ \mathrm{GeV^2 cm^{-5}}$

Predicted $t\bar{t}$ WIMP Annihilation Channel for the HAWC Observatory

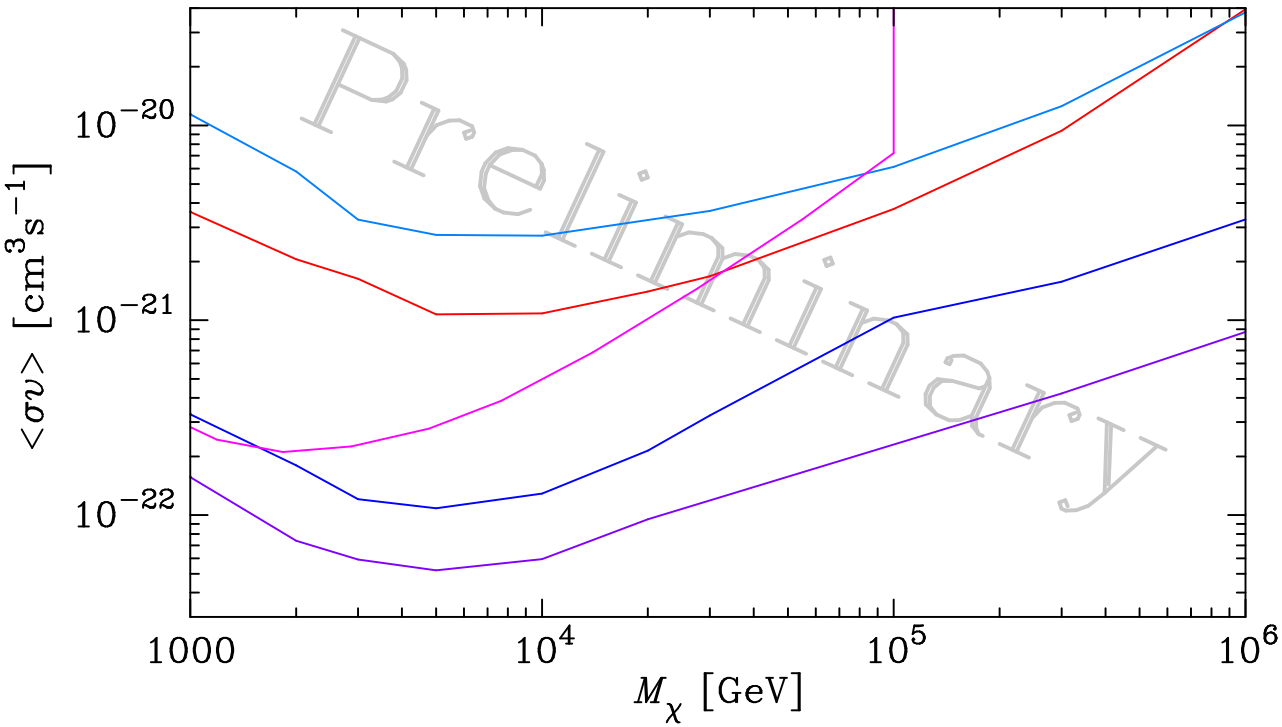

Pink line from HESS Observations of Sculptor for a $b\bar{b}$ spectrum from Viana 2011

Light blue line is limit from Draco

Red line is limit from Coma Berenices

Dark blue line is limit from GC with Einasto Profile

Purple line is limit from GC with NFW Profile

Cherenkov Telescope Array

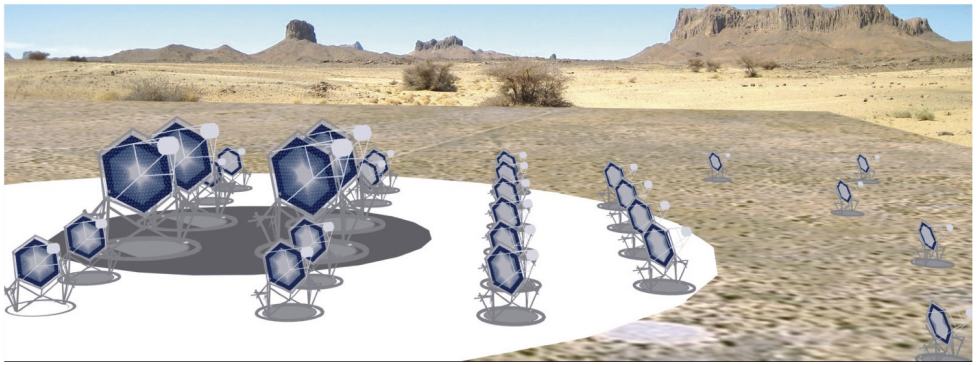

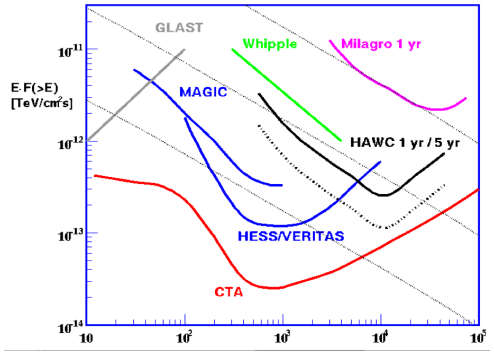

A few very large telescopes (20-30m) for low energies (< 100 GeV)

Grid of medium-sized telescopes (10-15m) for 0.1 - 10 TeV

Wide-spaced grid of small telescopes ($\sim$few m) for > 10 TeV

Southern site to observe the GC, with the highest energy threshold

Northern site to study AGN and star formation/evolution

Summary

- The Fermi-LAT Diffuse Gamma-Ray Background (DGRB) is one of the most stringent, yet robust, conservative constraints on WIMP-like dark matter.
- The DGRB is consistent with being produced by blazars with an evolving SED sequence model, plus emission from non-blazar AGN
- Resolution of the DGRB into blazars with further exposure in Fermi-LAT will enhance the sensitivity to WIMP like dark matter by a factor of 2 - 3 (95% CL)
- The Fermi-LAT has begun to exclude thermal dark matter for low masses
- HESS GC observation provides the strongest DM annihilation constraints for $M_\chi \gtrsim 900\ \mathrm{GeV}$.
- Future experiments, including HAWC and CTA, will probe the dark matter to mass scales and sensitivities well beyond the current reach

Fermi-LAT Positron Excess

Ackermann et al. 2011

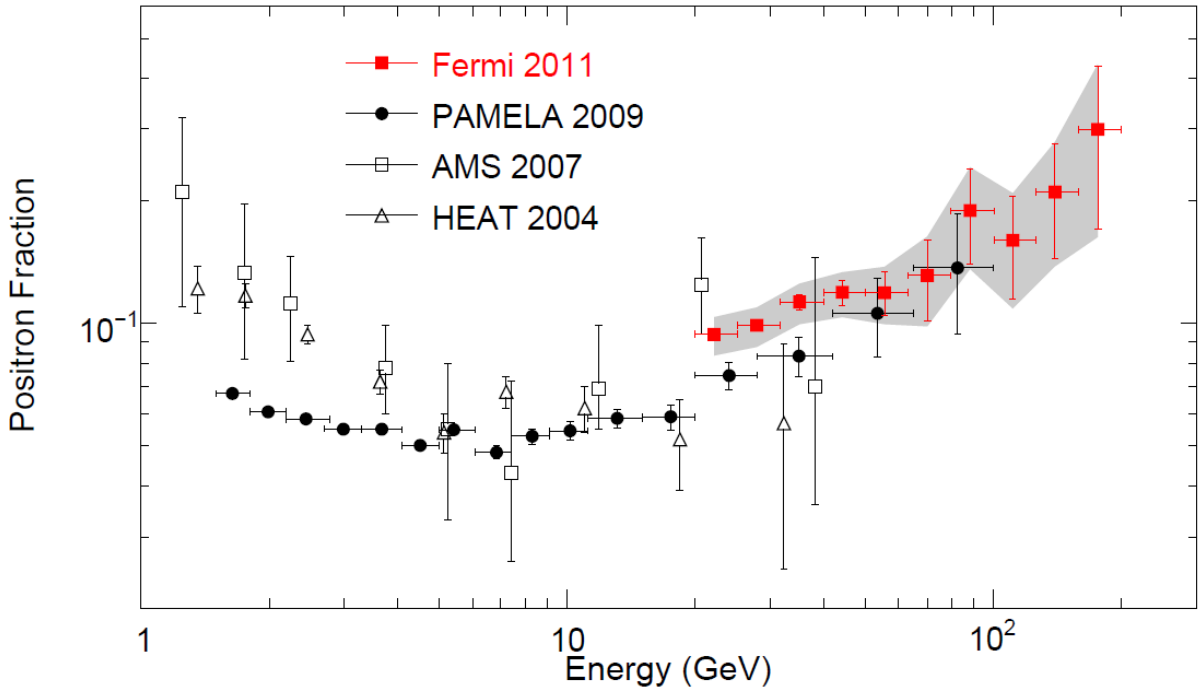

Diffuse Flux from Non-blazar AGN

- Comptonization of thermal electrons and nonthermal electrons from AGN coronae

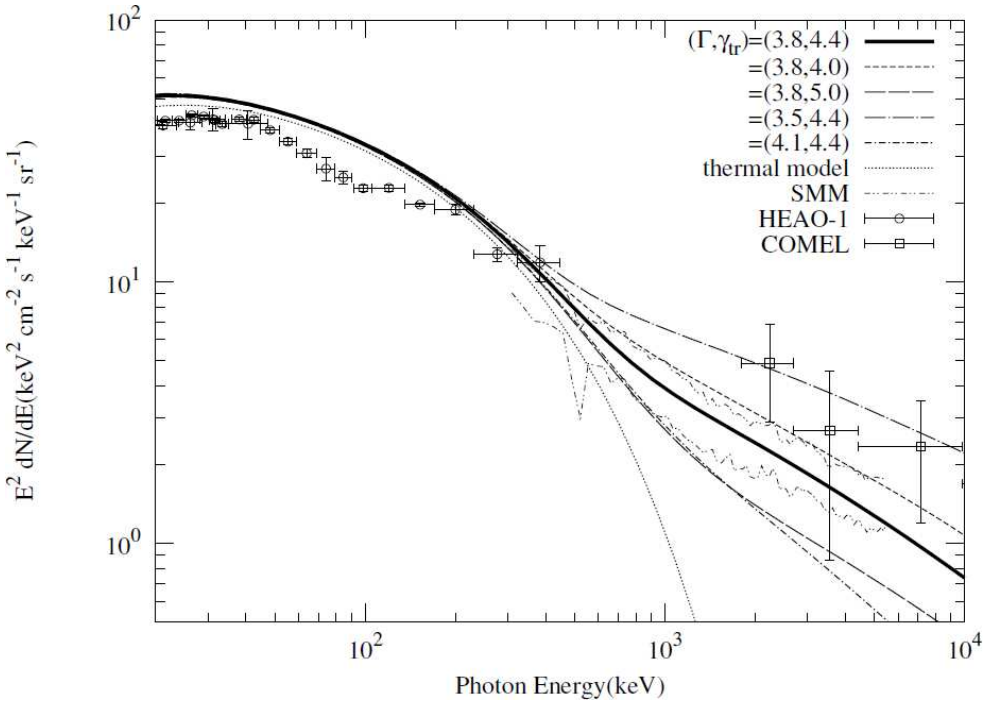

Figure: model from Inoue et al. (0709.3877)

GLF model

- $\rho_\gamma(L_\gamma, z) = \kappa \frac{dL_X}{dL_\gamma} \rho_X(L_X, z)$
- $\rho_X(L_X, z) = \rho_X(L_X, 0) f(L_X, z)$
- $\rho_X(L_X, 0) = \frac{A_X}{L_X ln(10)} \left[\left(\frac{L_X}{L_X^*} \right)^{\gamma_1} + \left(\frac{L_X}{L_X^*} \right)^{\gamma_2} \right]^{-1}$

$$f(L_X, z) = \begin{cases} (1+z)^{p_1} & z \leq z_c(L_X) \\ (1+z_c(L_X))^{p_1} \left(\frac{1+z}{1+z_c(L_X)} \right)^{p_2} & z > z_c(L_X) \end{cases}$$

$$z_c(L_X) = \begin{cases} z_c^* & L_X \geq L_a \\ z_c^* (L_X / L_a)^{\alpha} & L_X < L_a \end{cases}$$

GLF Parameters

Parameters for Ueda et al. (astro-ph/0308140)	
A_X	5.04×10^{-6} Mpc^{-3}
$log_{10} L_X^*$	$43.94^{+0.21}_{-0.26}$
γ_2	2.23 ± 0.13
z_c^*	1.9, fixed
$log_{10} L_a$	44.6, fixed
α	0.335 ± 0.07
p_1	4.23 ± 0.39
p_2	-1.5, fixed

Luminosities are in erg/s

SED Model 1

- SED is function of $\psi_R \equiv \psi(x = 9.698)$ and $x \equiv \log(\nu_{rest}/\ \mathrm{Hz})$
- $\psi(x;\psi_R) \equiv \log_{10}[\frac{\nu L_\nu(\nu(x),P(\psi_R))}{\mathrm{ergs}^{-1}}]$
- $\psi(x) = \log_{10}[10^{\psi_s(x)} + 10^{\psi_c(x)}]$
- $\psi_{s1}(x) \equiv (1-\alpha_s)(x - x_R) + \psi_R\ (x < x_{tr,s})$
- $\psi_{c1}(x) \equiv (1-\alpha_c)(x - x_X) + \psi_X\ (x < x_{tr,c})$
- $\alpha_s = 0.2,\ \alpha_c = 0.6,\ x_R = 9.698,\ x_X = 17.383$

$$\psi_X = \begin{cases} (\psi_R - 43) + 43.17 & \psi_R \leq 43 \\ 1.40(\psi_R - 43) + 43.17 & 43 < \psi_R \leq 46.68 \\ 1.40(46.68 - 43) + 43.17 & \psi_R > 46.68 \end{cases}$$

SED Model 2

- $\psi_{s2}(x) \equiv \psi_{s,p} - [(x - x_s)/\sigma]^2 \ (x \geq x_{tr,s})$
- $\psi_{c2}(x) \equiv \psi_{c,p} - [(x - x_c)/\sigma]^2 \ (x \geq x_{tr,c})$
- $\psi_{s,p} = (1 - \alpha_s)(x_{tr,s} - x_R) + \psi_R + \left(\frac{x_{tr,s} - x_s}{\sigma}\right)^2$
- $x_{tr,c} = \frac{-\zeta - \sqrt{\zeta^2 - 4\eta}}{2}$ $\zeta = \sigma^2(1 - \alpha_c) - 2x_c$
  $\eta = x_c^2 + \sigma^2[\psi_X - x_X(1 - \alpha_c) - \psi_{c,p}]$
- $x_{tr,s} = 10.699$, $x_c = x_s + 8.699$

SED Model 3

$$x_s = \begin{cases} -0.88(\psi_R - 43) + 14.47 & \psi_R \leq 43 \\ -0.40(\psi_R - 43) + 14.47 & \psi_R > 43 \end{cases}$$

$$\sigma = \begin{cases} 0.0891 x_s + 1.78 & \psi_R \leq 43 \\ [2(x_s - x_{tr,s})/(1 - \alpha_s)]^{1/2} & \psi_R > 43 \end{cases}$$

$$\psi_{c,p} = \begin{cases} \psi_{s,p} & \psi_R \leq 43 \\ 1.77(\psi_R - 43)^{0.718} + 45.3 & \psi_R > 43 \end{cases}$$

HESS Canonical WIMP Channels

Abazajian and JPH 2011

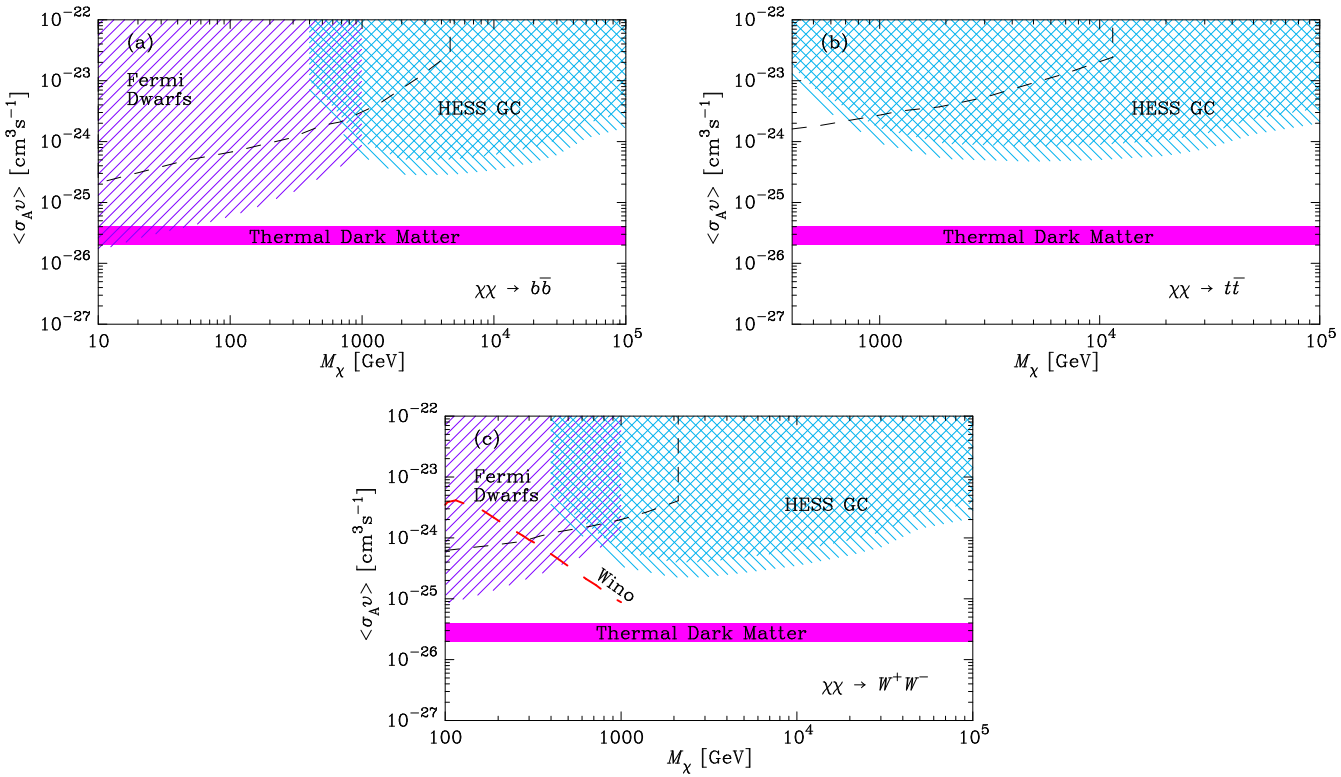

Fermi dwarf regions from Ackermann et al. 2011

Nonthermal Wino line from Grajek et al. 2008

Dashed Fermi-LAT 3σ limits from inner $3^\circ \times 3^\circ$ of MW from Cirelli et al. 2010

HESS Leptonic Annihilation Channels

Abazajian and JPH 2011

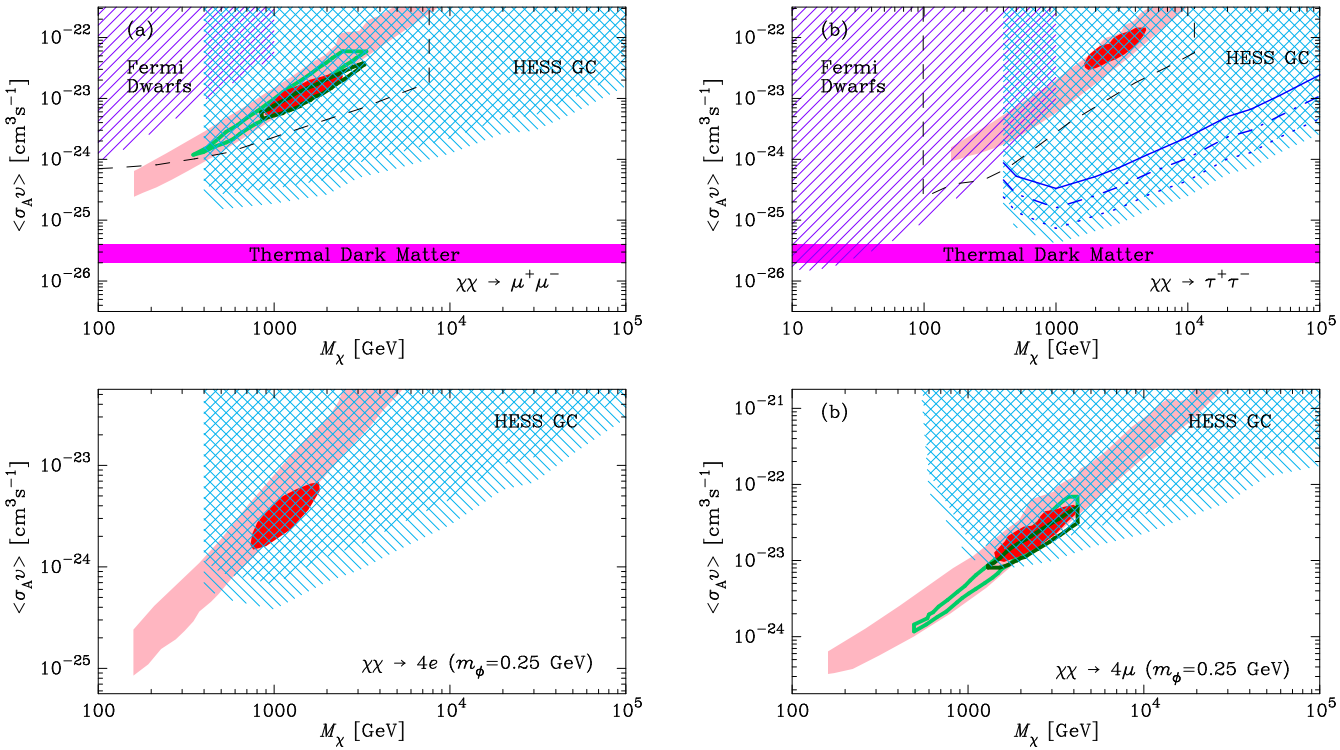

Pink (red) PAMELA (Fermi-LAT) excess regions from Mead et al. 2010

Light green (dark green) PAMELA (Fermi-LAT) excess regions from Bergstrom et al. 2009

Fermi dwarf regions from Ackermann et al. 2011

Dashed Fermi-LAT 3σ limits from inner $3^\circ \times 3^\circ$ of MW from Cirelli et al. 2010

HESS XDM Annihilation Channels

Abazajian and JPH 2011

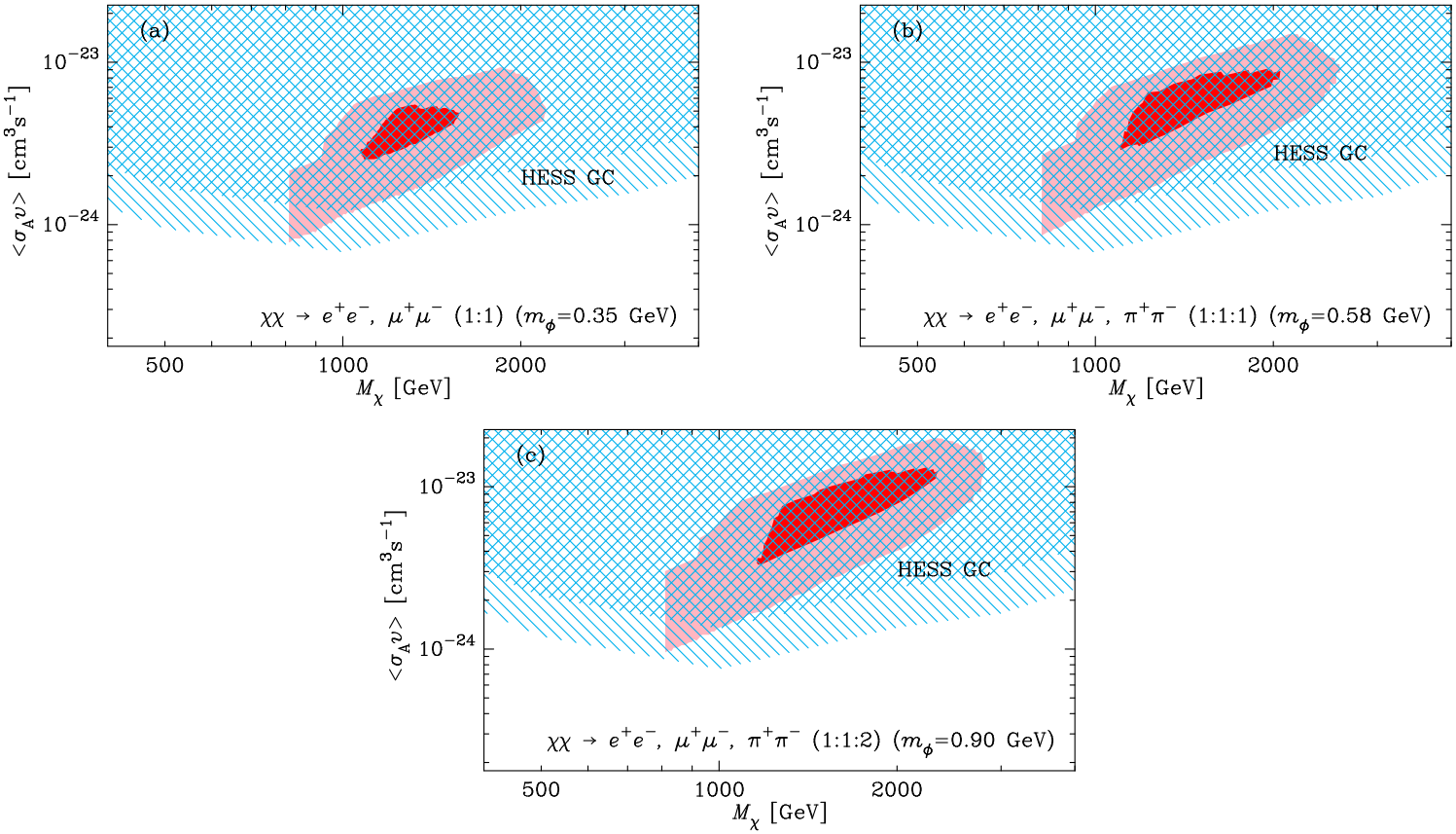

Pink (red) regions consistent at 68% CL (95% CL) with a combined

PAMELA + Fermi-LAT excess from Finkbeiner et al. 2010